Accelerated UV Testing and Characterization of PV Modules with UV-cut and UV-pass EVA Encapsulants

by

Kshitiz Dolia

A Thesis Presented in Partial Fulfillment
of the Requirements for the Degree
Master of Science

Approved April 2018 by the
Graduate Supervisory Committee:

Govindasamy Tamizhmani, Co-Chair
Matthew Green, Co-Chair
Devarajan Srinivasan

ARIZONA STATE UNIVERSITY

May 2018

ABSTRACT

Encapsulant is a key packaging component of photovoltaic (PV) modules, which protects the solar cell from physical, environmental and electrical damages. Ethylene-vinyl acetate (EVA) is one of the major encapsulant materials used in the PV industry. This work focuses on indoor accelerated ultraviolet (UV) stress testing and characterization to investigate the EVA discoloration and delamination in PV modules by using various non-destructive characterization techniques, including current-voltage (IV) measurements, UV fluorescence (UVf) and colorimetry measurements. Mini-modules with glass/EVA/cell/EVA/backsheet construction were fabricated in the laboratory with two types of EVA, UV-cut EVA (UVC) and UV-pass EVA (UVP).

The accelerated UV testing was performed in a UV chamber equipped with UV lights at an ambient temperature of 50°C, little or no humidity and total UV dosage of 400 kWh/m^2. The mini-modules were maintained at three different temperatures through UV light heating by placing different thickness of thermal insulation sheets over the backsheet. Also, prior to thermal insulation sheet placement, the backsheet and laminate edges were fully covered with aluminum tape to prevent oxygen diffusion into the module and hence the photobleaching reaction.

The characterization results showed that mini-modules with UV-cut EVA suffered from discoloration while the modules with UV-pass EVA suffered from delamination. UVf imaging technique has the capability to identify the discoloration region in the UVC modules in the very early stage when the discoloration is not visible to the naked eyes, whereas Isc measurement is unable to measure the performance loss until the color

becomes visibly darker. YI also provides the direct evidence of yellowing in the encapsulant. As expected, the extent of degradation due to discoloration increases with the increase in module temperature. The Isc loss is dictated by both the regions – discolored area at the center and non-discolored area at the cell edges, whereas the YI is only determined at the discolored region due to low probe area. This led to the limited correlation between Isc and YI in UVC modules.

In case of UVP modules, UV radiation has caused an adverse impact on the interfacial adhesion between the EVA and solar cell, which was detected from UVf images and severe Isc loss. No change in YI confirms that the reason for Isc loss is not due to yellowing but the delamination.

Further, the activation energy of encapsulant discoloration was estimated by using Arrhenius model on two types of data, %Isc drop and ΔYI. The Ea determined from the change in YI data for the EVA encapsulant discoloration reaction without the influence of oxygen and humidity is 0.61 eV. Based on the activation energy determined in this work and hourly weather data of any site, the degradation rate for the encaspulant browning mode can be estimated.

To,

My father, mother, and brother, for their unconditional love, unending support and unwavering belief in me.

I hope I do you'll proud.

ACKNOWLEDGMENTS

I would like to express my sincere gratitude to Dr. Govindasamy Tamizhmani for providing me with the opportunity to work on this study. It was due to your continuous support and guidance that I was able to achieve my goals. Thank you for always inspiring me to try a different approach whenever the experiments were not going the right way.

I would also like to thank Dr. Green and Dr. Srinivasan to extend their support to my research. I would like to specially thank my project supervisor, Dr. Archana Sinha for always being there to support me throughout the research. I would like to show my gratitude to Shashwata Chattopadhyay for helping me with the inception of this research work. I would never have achieved this feat without the support from my PRL colleagues. I would like to thank Sai Tatapudi for helping me with technical aspects of various equipment at the lab. I would also like to thank Hamsini Gopalakrishna for providing different perspective in various scenarios. Finally, I would take this opportunity to thank former students of PRL whose work laid the foundation for my research.

TABLE OF CONTENTS

Page

LIST OF TABLES vii
LIST OF FIGURES viii
CHAPTER
1 INTRODUCTION 1
1.1 Background 1
1.2 Statement of the Problem 6
1.3 Thesis Objective 7
2 LITERATURE REVIEW 8
3 METHODOLOGY 14
3.1 Module Construction 14
3.2 Accelerated UV stress testing 15
3.3 Module Fabrication 20
3.3.1 Module Lamination 20
3.4 Characterization Techniques 22
3.4.1 IV Measurement 22
3.4.2 UV Fluorescence Imaging 23
3.4.3 Colorimetry Measurement 24
3.5 Model for Activation Energy Estimation 25

CHAPTER PAGE

4 RESULTS AND DISCUSSION 27

4.1 UV Fluorescence Results 27

4.2 IV Results 31

4.3 Colorimetry Results 33

4.4 Correlation between Isc and YI 38

4.5 Activation Energy Determination 40

3.6.1 Activation Energy Calculation from Isc Drop 41

3.6.2 Activation Energy Calculation from YI Data 42

5 CONCLUSIONS 44

REFERENCES 48

LIST OF TABLES

Table Page

4-1: Characterization results for center cell of all UVC modules 36

4-2: Characterization results for center cell of all UVP modules 37

5-1: Characterization results for center cell of all UVC modules 46

5-2:Characterization results for center cell of all UVP modules 47

LIST OF FIGURES

Figure Page

1.1: Causes and effects of encapsulant discoloration 3

1.2: The chemical reaction process indicating the activation energy [8] 4

2.1: UV induced degradation mechanism[12] 8

2.2: Schematic diagram of degradation pathways of the yellowing process in an EVA-encapsulated PV module [6]. 10

2.3: Causes and effects of delamination 13

3.1: Outside view of the UV chamber 15

3.2: Inside view of a) unlighted UV chamber b) lighted UV chamber 16

3.3: Top-view of the six mini-modules 17

3.4: Rear view of mini-module with aluminum tape attached on the backsheet 17

3.5: Front view of mini-module with sealed edges 18

3.6: Side view of mini-module with sealed edges 18

3.7: Mini-modules arranged on the rack placed inside the walk-in UV chamber 19

3.8: Mini-modules with different thickness of insulation attached on the backsheet 19

3.9: Laminator with the cover open 21

3.10: Laminator with the control system 21

3.11: Cell numbering scheme in the 9-cell mini-modules (cell pieces cut from a single cell) 22

3.12: (a) Schematic of UVF imaging set-up with two UV light source arrays angled towards the module. The module emits visible light. (b) Photograph of the set-up with the UV arrays 24

3.13: Colorimetry setup with a) placing the spectral radiometer and b) taking measurement 25

Figure Page

4.1: UVf images of UVC mini-modules at different temperatures and UV dosage levels under accelerated UV testing. 28

4.2: UVf images of UVP mini-modules at different temperatures and UV dosage levels under accelerated UV testing. 29

4.3: Close-up UVf images of center cell from UVC-3 (high temperature) and UVP-3 (high temperature) modules 30

4.4: IV curve for UVC-3 cell 2 at various stages of accelerated stress test (0, 200 and 400 kWh/m^2 UV dosage) 32

4.5: IV curve for UVP-3 cell 2 at various stages of accelerated stress test (0, 200 and 400 kWh/m^2 UV dosage) 32

4.6: Percent Isc degradation of mini-modules after 400 kWh/m^2 UV exposure in the chamber testing at low (UVC 1, UVP 1), mid (UVC 2, UVP 2) and high (UVC 3, UVP 3) temperatures. .. 33

4.7: ΔYI values for cells of different UVC modules along with control module (UVC 1 low temperature; UVC 2 mid temperature; UVC 3 high temperature) 34

4.8: ΔYI values for cells of different UVP modules along with control module (UVP 1 low temperature; UVP 2 mid temperature; UVP 3 high temperature) 35

4.9: ΔYI of mini-modules after 400 kWh/m^2 UV exposure in the chamber testing at low (UVC 1, UVP 1), mid (UVC 2, UVP 2) and high (UVC 3, UVP 3) temperatures. 35

4.10: Isc vs YI plot for UVC modules at various stages of the accelerated stress test 39

4.11: Isc vs YI plot for UVP modules at various stages of the accelerated stress test 40

4.12: Variation of ln(Isc drop(%)) of UVC modules with inverse of temperature. Activation energy is calculated from the slope of linear fit on degradation data at three different temperatures. 41

Figure Page

4.13: Variation of ln(ΔYI) of UVC modules with inverse of temperature. Activation energy is calculated from the slope of linear fit on degradation data at three different temperatures. 42

1 INTRODUCTION

1.1 Background

The solar photovoltaic (PV) is one of the major renewable energy sources, whose usage has increased tremendously in the past decade. The continuous research in the field has reduced PV module price over the years, which has caused huge penetration of this technology in the market. The focus, in the beginning, was on increasing the power of a PV module but in recent years a significant research is being done for increasing the safety and reliability of PV modules.

The PV module consists of a semiconductor (solar cell) which absorbs photons from sunlight to generate electron-hole pairs that further flow in a circuit to produce electricity. There are various types of photovoltaic technologies in the market- crystalline silicon, amorphous silicon, thin film etc. The crystalline silicon currently dominates with about 90% market share. The PV module manufacturers claim a 25 years lifetime for crystalline silicon modules which means that the PV module should perform at a minimum efficiency of 80%. But, module efficiency loss of more than 20% was seen in many modules which raised the question of reliability of these modules. This resulted in an increase in reliability research to address various degradation modes in the PV module.

A typical PV module undergoes various degradation modes during its operational lifetime like encapsulant browning, solder bond degradation, corrosion, delamination etc. The encapsulant browning is one of the most common encapsulant degradation in field-

deployed modules, especially in hot climates. Suleske reported a browning defect in 89.4% of 1865 modules deployed at APS-STAR, Phoenix[1].

The functions of an encapsulant in a PV module are to provide structural support to the solar cell, maintain maximum optical coupling between the solar cell and incident solar irradiation, provide physical isolation of solar cell and circuit from degrading environmental factors e.g. hail, soil, provide electrical isolation to the solar cell circuit and to support the interconnects and other electrical connections[2][3]. Various additives are added in the polymer composition to protect the solar cell. UV absorbers (UVA), UV light stabilizers (UVS), and antioxidants (AO) are commonly added to the polymer to reduce its degradation rate and improve their service life. The primary function of UVA is to absorb the UV light and dissipate its energy as heat or re-emit it as unharmful light of longer wavelength. The UVA itself may be lost in this process. The UVS acts as a free radical scavenger to neutralize free radicals generated in the polymeric matrix. The AO is used to reduce the extent of thermal oxidation during thermal processing and to decompose peroxides and hydroperoxides in the polymer[4].

Over time, a wide variety of encapsulant materials have been used in modules- polyvinyl butyral (PVB), ethylene-vinyl-acetate (EVA), silicone rubber, ionomers, and more recently polyolefins (POE)[5][6]. The EVA is the most commonly used encapsulant in PV industry due to its low cost. But, it has been observed in the field that it turns brown over a period which decreases the transmission of photons to the solar cell. This causes the loss of short

circuit current (Isc) and in turn, efficiency, as fewer photons contribute to the generation of electricity from PV modules.

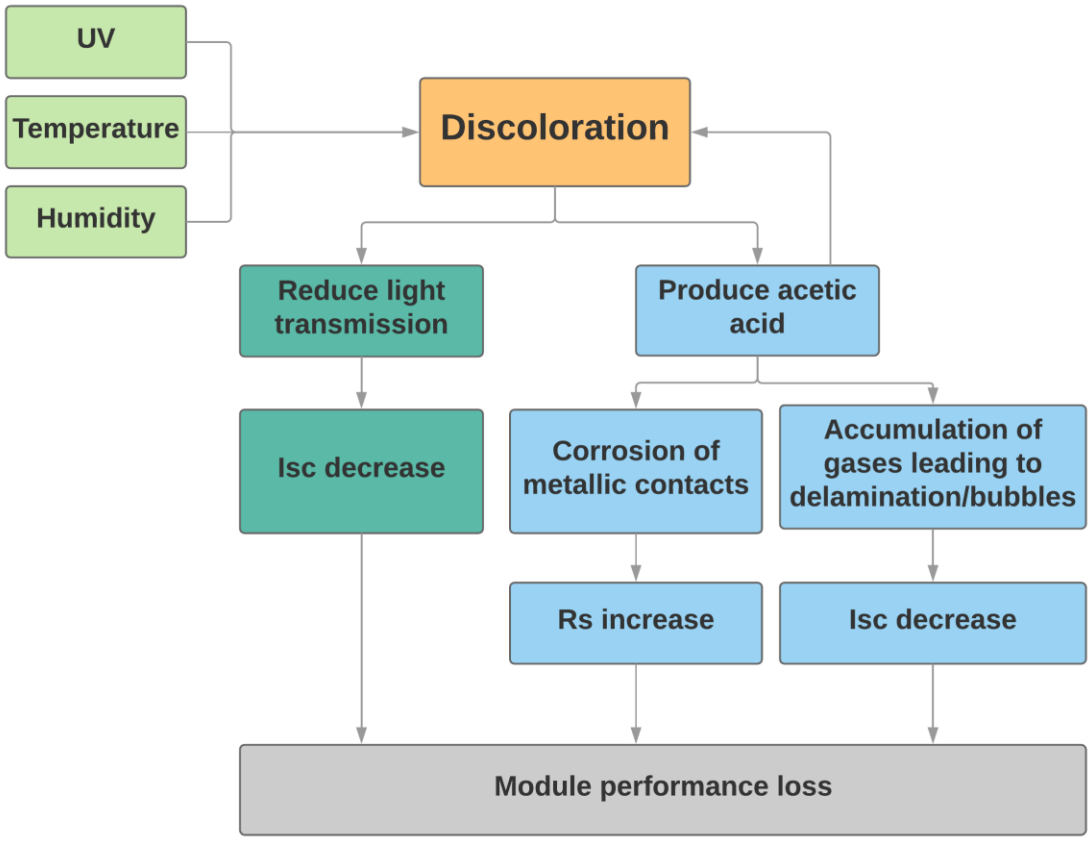

Figure 1.1: Causes and effects of encapsulant discoloration

In the PV module encapsulant, two reactions having opposing effects occur simultaneously which affect the degradation rate. These reactions are encapsulant browning and photobleaching. The encapsulant browning occurs due to the loss of additives present in the EVA, particularly UV absorber under the action of UV light and high temperature.

The photobleaching reaction essentially occurs in the presence of oxygen and light. The oxygen enters the module through breathable backsheet and diffuses into the EVA and breaks down the polyconjugates in the colored chromophores[7]. At the edge of the cell, the photobleaching reaction dominates over the browning reaction and so we see a colorless EVA at the edge of the cell. But due to diffusion limitation of oxygen in the EVA, the amount of oxygen diffusing towards the center of cell keeps on reducing. Due to this reason, the browning reaction dominates in the region closer to the center of the cell.

In PV reliability context, the activation energy (E_a) refers to the minimum amount of energy required to initiate the temperature accelerated degradation. The focus of this thesis is to find out the activation energy for encapsulant browning. But, as both photobleaching and browning reaction occur simultaneously, some changes were made in the setup to eliminate photobleaching reaction so that primarily only browning reaction could occur.

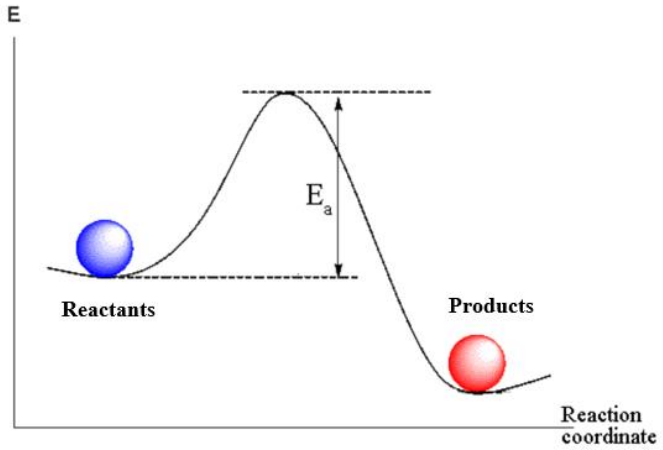

Figure 1.2: The chemical reaction process indicating the activation energy [8]

The EVA available in the market from different manufacturers has different amount and type of additives. Also, there are primarily two kinds of EVA available in the market, based on its action on UV light- UV-cut EVA and UV-pass EVA. The UV-cut EVA particularly contains some additive known as UV absorber which absorbs UV light below 360 nm and protects the cell and backsheet from its harmful effects. The amount of UV absorber reduces over time as it undergoes photodegradation and curing to form UV excitable chromophores[4]. On the other hand, UV-pass EVA does not have absorber in its composition and so allows UV light to penetrate the cell as well as the backsheet.

The PV module manufacturers provide a 20-25 years warranty which claims less than 20% loss in efficiency during this period. It is not feasible to wait for 20-25 years to study degradation in PV modules. This called for the development of an accelerated stress testing which can closely simulate the field degradation of PV modules. The various factors which affect the efficiency of the module were identified and they were used to accelerate the degradation in PV modules. These tests provide valuable information regarding the rate of degradation and its relationship with various parameters present in the field. In this thesis accelerated UV stress testing was done to study/investigate degradation in different types of EVA in PV modules.

To analyze the performance of a PV module, various characterization could be performed. Characterization techniques are broadly classified into two sets: destructive and non-destructive methods. The non-destructive characterizations provide valuable information about the drop in performance of PV modules at different stages of degradation without

destroying the sample hence this technique allows the continuation of the stress test on same PV modules[9][10]. The destructive characterization allows to detect changes in the composition of the material at a more fundamental level and is very useful. It is suggested to perform at the end of the accelerated stress test. Thermogravimetric analysis (TGA), Dynamic scanning colorimetry (DSC), Fourier transform infrared spectroscopy (FTIR) and Raman spectroscopy are some of the destructive characterizations while IV measurement, UV fluorescence imaging, Colorimetry, Electroluminescence imaging, Infrared imaging are some of the non-destructive characterizations. Among these, Electroluminescence and Infrared imaging are generally done to analyze PV modules for solder bond degradation, hotspots identification and other electrical degradations. This thesis focuses on the non-destructive characterization of mini-modules with UV-cut and UV-pass EVA and recommends doing destructive characterization at the end of the accelerated stress test. The destructive characterizations are not in the scope of this study.

1.2 **Statement of the Problem**

Past studies of EVA were done to determine the mechanism behind its yellowing with field exposure. Various tests were designed to capture different aspects of it and to provide further evidence of the mechanism. The EVA formulation was changed multiple times to reduce or slow-down the yellowing. This study compares two EVA types- UV-cut EVA and UV-pass EVA to see different degradation types.

1.3 Thesis Objective

The main objectives of this study are as follows:

- Performing accelerated UV testing and characterizations on mini-modules with UV-cut and UV-pass EVA to find out the different degradation modes in them.
- Finding the factors which affect the calculation of activation energy for encapsulant browning.
- Developing multiple techniques to estimate the activation energy for encapsulant browning.

2 LITERATURE REVIEW

EVA is the most commonly used encapsulant in c-Si PV modules. It is a random copolymer consisting of about 67 wt% polyethylene and 33 wt% polyvinyl acetate[11]. The EVA undergoes thermal and photochemical degradation to form chromophores (conjugated moieties capable of absorbing visible light) which can show strong fluorescence and cause yellowing of EVA. This is accompanied by the formation of volatile compounds such as hydroperoxides and acetic acid as degradation products (*Figure* Figure *2.1*) [12].

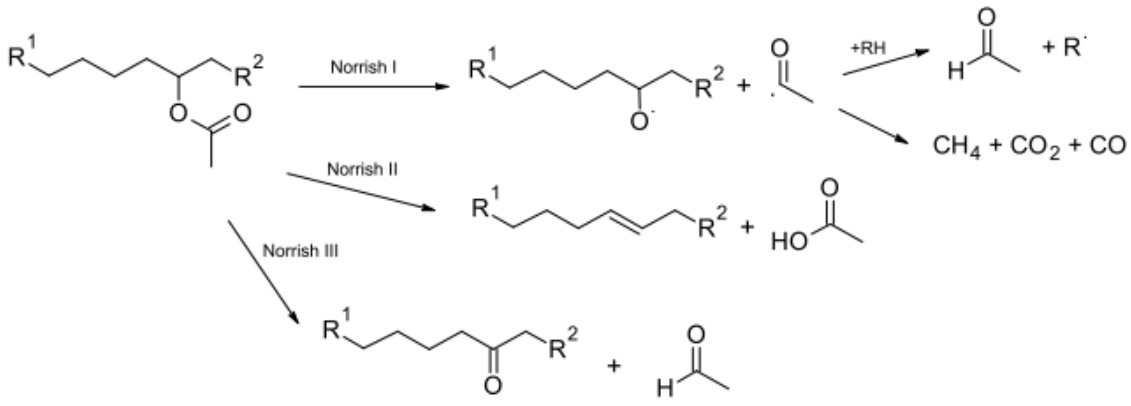

Figure 2.1: UV induced degradation mechanism[12]

Acetic acid is formed at temperatures between 120 to 150°C which could be reached during polymerization and palletisation of EVA copolymer, film extrusion and PV module lamination and it further catalyzes the initial de-acetylation reaction[13]. The acetic acid gets accumulated in front of the solar cells due to long diffusion paths between encapsulant and backsheet. The acetic acid lowers the local pH in front of the cells which causes faster corrosion of cell metallization[14].

The peroxide catalyst which acts as a crosslinking agent is depleted during lamination of the module[15]. Faster curing during the lamination process could cause incomplete/inadequate crosslinking of polymer which may lead to the presence of residual peroxide catalyst which can take part in UV-initiated photochemical reaction[6]. The formation of chromophores takes place due to degradation of peroxide additive left after curing of the module. To avoid UV absorption by these chromophores, UV absorbers were added to the EVA formulation. But the UV absorber itself is prone to UV-induced photo degradation which leads to decrease in its absorbance[4].

Another additive, hindered amine light stabilizer (HALS) is added to the EVA formulation to eliminate reactive free radicals and stabilize the UV absorber under the action of UV and oxygen[16][17]. The oxygen diffuses to the module encapsulation in case of breathable polymer backsheet but the diffusion through the encapsulant is usually slow. Pern has reported a drop in concentration of UV absorber in UV exposed modules from the edge towards the center of the solar cell[4]. This may be due to the absence of oxygen towards the center of the cell which inhibits the action of HALS and hence leads to the degradation of UV absorber. The chromophore impurities absorb UV and form chromophores with longer conjugation lengths, which absorb radiation in longer wavelengths and lead to yellowing of the encapsulant. Therefore, oxygen diffusion may be the key for the conservation of UV absorber and hence for long time protection of the encapsulant from degradation[18][19].

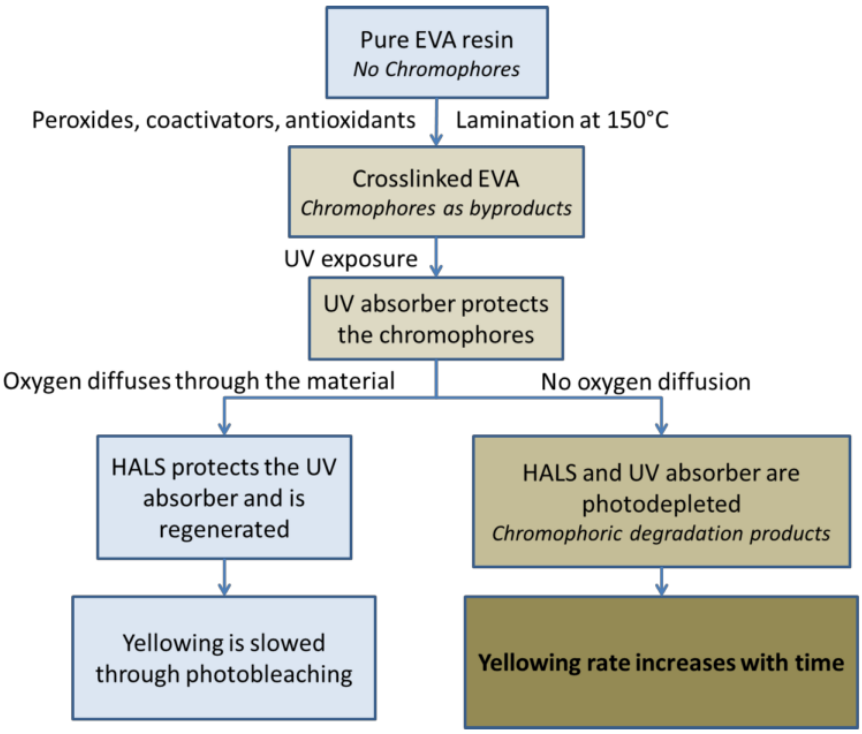

Figure 2.2: Schematic diagram of degradation pathways of the yellowing process in an EVA-encapsulated PV module [6].

Klemchuk et al. analyzed degradation in laboratory prepared EVA samples along with field-aged modules recovered from Carissa Plains, CA power plant and other installations. The reduction in vinyl acetate content in the polymer was not very significant which suggests little double bond formation from photolysis of vinyl acetate. The stabilizer contents were analyzed, and it was found that the discoloration in modules was mainly due to the degradation of UVA in the presence of another additive- peroxide which is added for curing of the PV module during lamination. The modules had Cyasorb UV-531 as the UV absorber and Lupersol-101 as the peroxide along with other additives[11].

David Miller et al. performed accelerated UV stress testing on various glass/EVA/glass specimens under various steady-state conditions to quantify the activation energy for encapsulant discoloration. The tests were done in two devices- i) Ci5000 by ATLAS Material Testing Technology LLC equipped with Xenon-arc lamp with "Right Light" filter and ii) NREL "UV Suitcase", a custom chamber equipped with UVA-340 fluorescent lamps. The Ci5000 used irradiance setting of 1 $W/m^2/nm$ at 340 nm, chamber temperature of 60°C and 30% relative humidity (RH). The UV Suitcase was set at irradiance setting of 1 $W/m^2/nm$ at 340 nm, chamber temperature of 60°C and uncontrolled RH. The tests were done in 3 chambers operating at different temperatures. The estimated activation energy for encapsulant browning after using Arrhenius fit on the data was ~60 kJ/mol (0.62 eV) [20].

Deepak Jain performed the accelerated UV stress test on MSX mini-modules in ATLAS Ci4000 weather-Ometer chamber, equipped with Xenon-arc lamp. The UV testing was performed at irradiance setting of 1 $W/m^2/nm$ at 340 nm, 65% RH and a chamber temperature of 20°C. The estimated activation energy for encapsulant browning lies in the range 26-44 kJ/mol (0.27-0.46 eV) [21].

The field data from various locations representing different climate types- cold and humid (New York) and cold and dry (Colorado) were compared with field data from hot and dry (Arizona) by Shantanu Pore. Arizona was considered as accelerated degradation climate in comparison with other climate types and the activation energy for encapsulant browning was estimated by first determining the acceleration factor from the ratio of Isc degradation

rate in Arizona and other climate types and then substituting in Modified Arrhenius model. The estimated activation energy for encapsulant browning was 0.3 eV [22].

Delamination is another major degradation mode observed in the field deployed PV modules. The major drivers for the delamination are- 1) the stress exerted at the interface from residual thermal stresses or from external mechanical stress applied on the module, 2) the deteriorated interfacial bonding due to attack from heat, UV and moisture. Delamination creates new interfaces- a) glass/air and air/EVA in case of glass/EVA delamination, b) EVA/air and air/cell front in case of cell front/EVA delamination[6]. Delamination causes the optical decoupling between the solar cell and encapsulant which reduces Isc. It also allows more accumulation of moisture and acetic acid which leads to corrosion of cell metallization. Sánchez-Friera et al. observed power loss of 11.5% in 12 years exposed PV modules due to delamination[23].

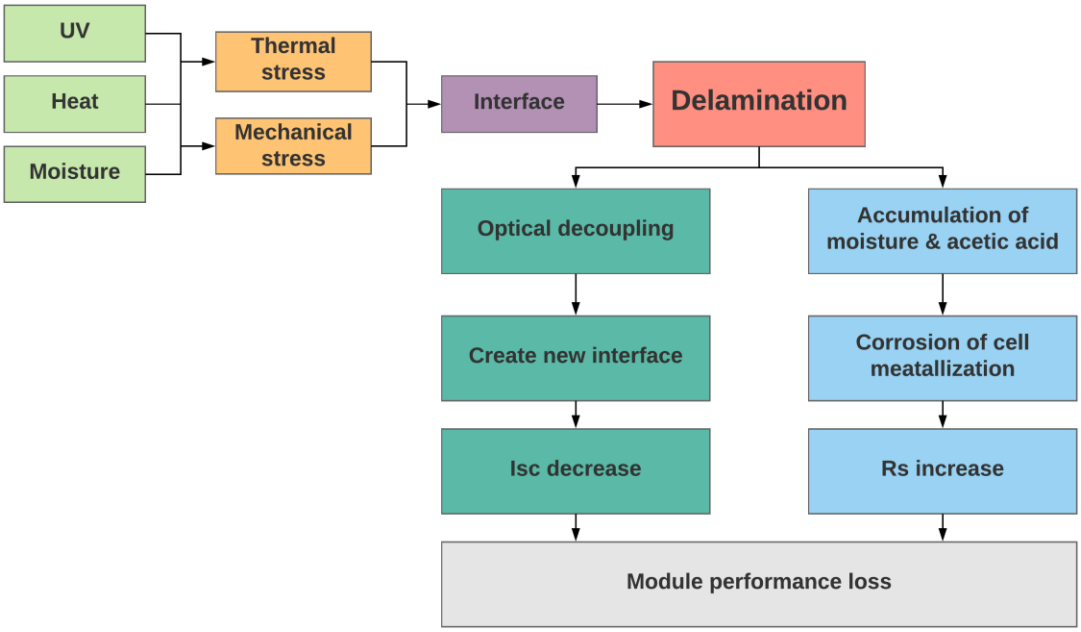

Figure 2.3: Causes and effects of delamination

Several studies have been done to develop a detection technique for the delamination in PV modules. Sinha et al. proposed a fast and non-destructive analysis method to detect delamination and estimate the delamination thickness based on pulse infrared thermography[24]. Voronko et al. performed a couple of non-destructive tests- pulse thermography and scanning acoustic microscopy (SAM), to detect several defects including delamination[25].

3 METHODOLOGY

3.1 Module Construction

The samples used for this study were eight lab-fabricated mini-modules of the representative glass/EVA/cell/EVA/ backsheet construction rather than glass/EVA/glass coupon construction conventionally used by the other researchers in their accelerated test setup[20]. Six mini-modules were put inside UV chamber for stress testing while remaining two mini-modules were used as control modules. The control module does not undergo any stress and is used to ensure the accuracy of measurement. The control module goes through the same measurements along with the samples and gives information about the measurement error in the method. The nine mono-Si cells in each mini-module were obtained by laser cutting of a single mono-Si cell. Each cell in each module is individually accessed through individual cell ribbons for performance measurements.

These mini-modules were categorized into two sets based on EVA type used to encapsulate the solar cells: UV-cut EVA (UVC) and UV-pass EVA (UVP). Four mini-modules have UV-cut EVA while other four have UV-pass EVA. This was done to see the degradation modes in both kinds of EVA. The UV-cut EVA absorbs UV light below 360 nm wavelength and protects the anti-reflection coating (ARC) of cells and the backsheet from severe degradation, whereas UV-pass EVA allows the transmission of UV light to the cell to slightly improve the cell performance at the risk of backsheet degradation.

The backsheet of mini-modules and the laminate edges were covered by wide aluminum tape to prevent the oxygen diffusion into the laminate. This approach retards the bleaching

action by oxygen and accelerates the browning degradation due to UV, temperature and possibly acetic acid generated during lamination and UV exposure. This was done to find activation energy for browning reaction only.

3.2 Accelerated UV Stress Testing

The accelerated UV stress testing was performed in a walk-in UV chamber equipped with rack housing for test samples. The UV chamber has a rack housing 144 UV tube lights in two rows and two fans on the roof for temperature control. The mini-modules were exposed to UV irradiance of 215 W/m^2 at a chamber temperature 50°C under dry heat. A UV sensor was placed inside the chamber in-plane to module surface to measure the UV irradiance intensity.

Figure 3.1: Outside view of the UV chamber

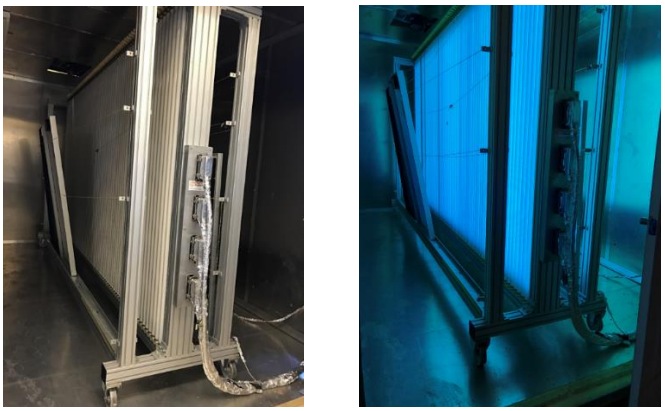

Figure 3.2: Inside view of a) unlighted UV chamber b) lighted UV chamber

A T-type thermocouple was attached on the backsheet (between backsheet and aluminum tape) behind the center cell of all the modules. By putting the thermocouple on the center cell, edge effects were removed which could cause variation across temperature readings of different modules. The module temperature was continuously monitored using a data acquisition system at an interval of one minute.

Three different module temperatures were achieved simultaneously in the same chamber by attaching an insulation material of varying thickness at the backsheet. The module temperatures achieved were- 64°C, 73°C, 78°C. This novel technique of achieving three different temperatures in a single chamber helps in reducing test time, cost and resources. In the past, researchers used to operate the chamber multiple times at different temperatures which consume a lot of time and the comparison of degradation could not be done until the test completes.

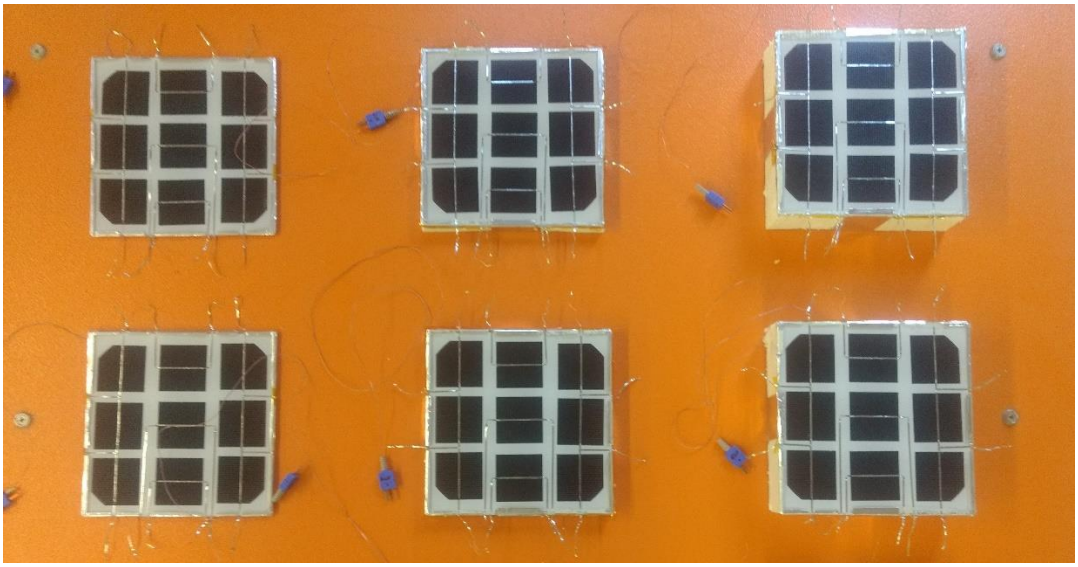

Figure 3.3: Top-view of the six mini-modules

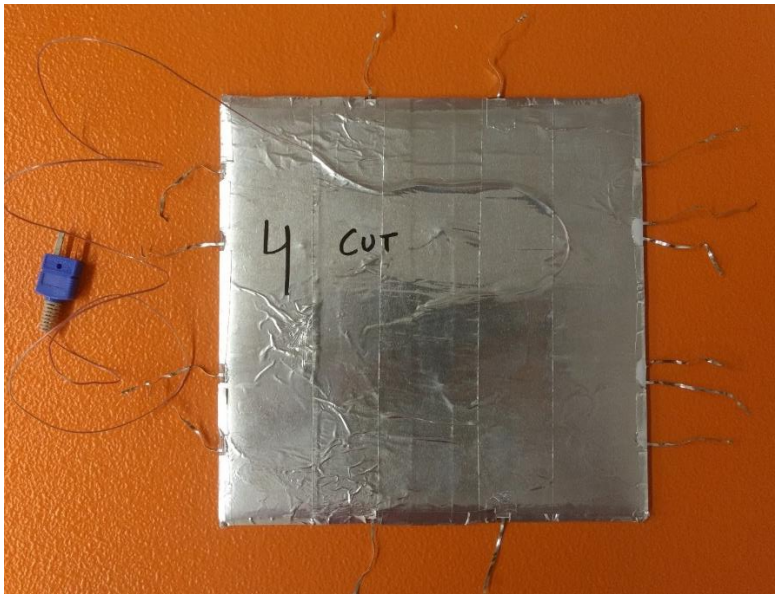

Figure 3.4: Rear view of mini-module with aluminum tape attached on the backsheet

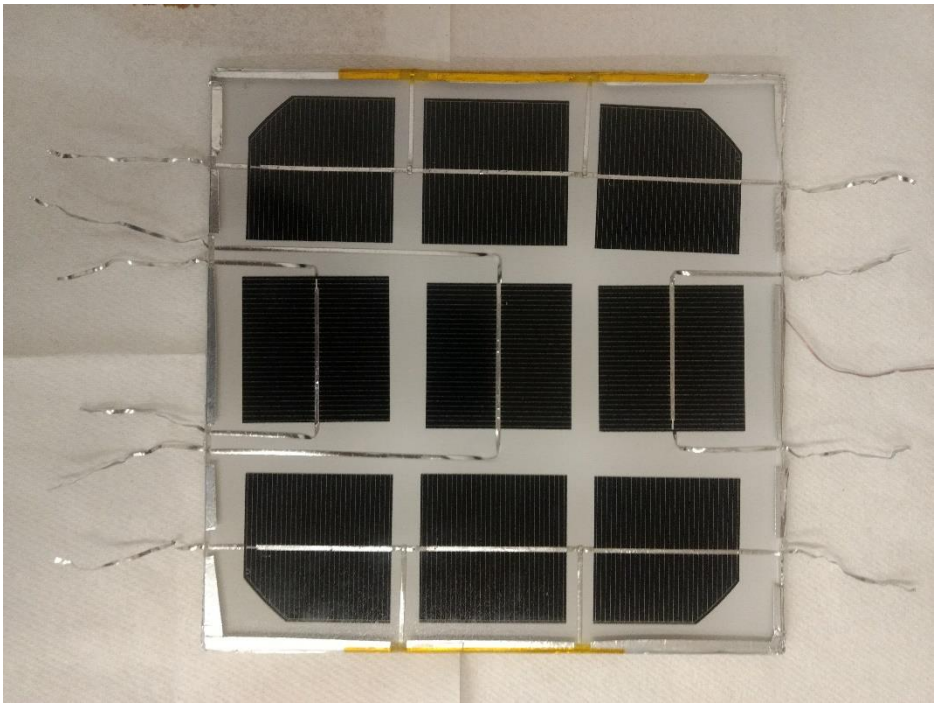

Figure 3.5: Front view of mini-module with sealed edges

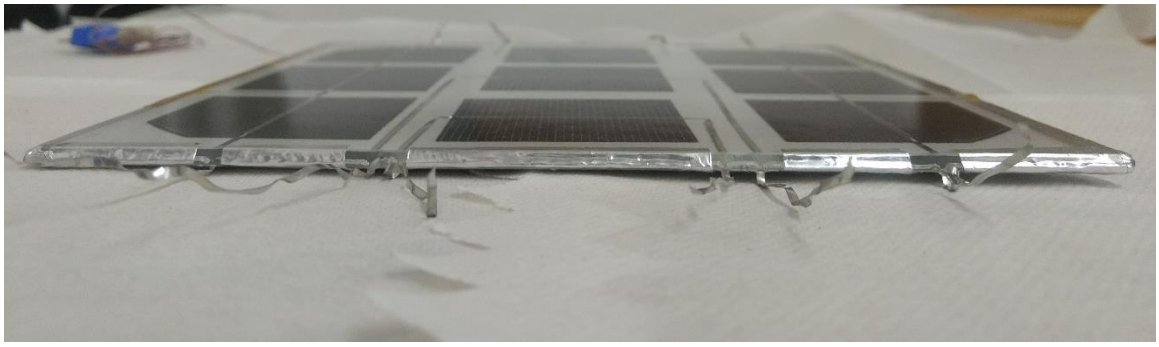

Figure 3.6: Side view of mini-module with sealed edges

Figure 3.7: Mini-modules arranged on the rack placed inside the walk-in UV chamber

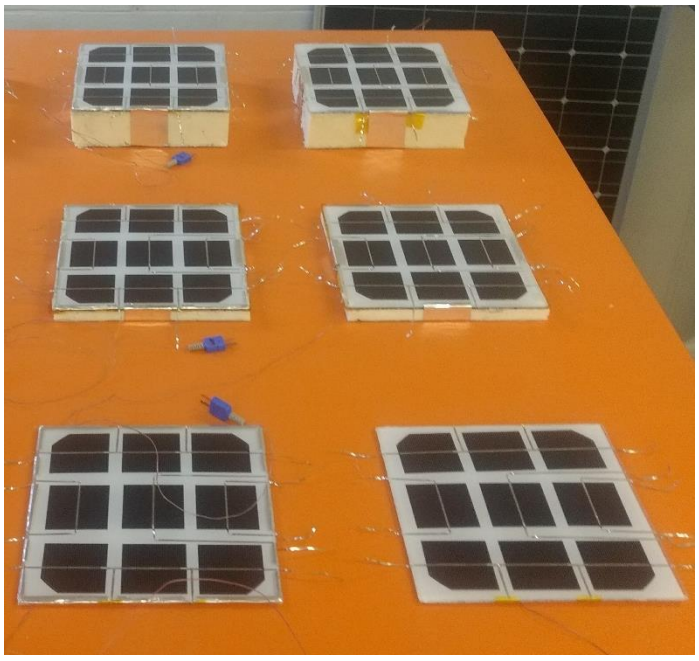

Figure 3.8: Mini-modules with different thickness of insulation attached on the backsheet

3.3 Module Fabrication

A good quality monocrystalline silicon cell of 156 x 156 mm^2 dimension was selected. The cell was cut into 9 pieces by using laser cutting technology at "Advotech Industries". Each cell piece is 52 x 52 mm^2. These cell pieces were then soldered to ribbon using soldering machine. Two different kinds of EVA, UV-cut and UV-pass, were used for encapsulation system. Tedlar-Polyester-Tedlar (TPT) backsheet was used at the back while a tempered glass of 8 x 8 $inches^2$ dimension from Solite was used at the front. The distance between cell edge and module edge was 11-12 mm. The inter-cell distance was 11-12 mm.

3.3.1 Module Lamination

The layers were stacked up in the following order to laminate the mini-modules. Textured side of glass facing up, encapsulant with the smooth side down, the nine cell pieces (with interconnect ribbons) properly arranged with the backside facing up, encapsulant with the smooth side down, outside of the backsheet facing up. The stacking up process is same for all the mini-modules, except the encapsulant- UV-cut EVA for UVC and UV-cut EVA for UVP. This stacked up arrangement was kept in between two polytetrafluoroethylene (PTFE) sheets and then placed inside the laminator as shown in *Figure* Figure *3.9*. The lamination was performed at a temperature of 150 °C under vacuum for nearly 20 minutes. After the lamination process completes, the mini-modules were allowed to cool down for 10 minutes before removing from the laminator.

The samples used to study encapsulant browning in past researches[20] were small coupons in which encapsulant is laminated between two glass pieces rather than actual

solar cell along with all other components of a module. In this research, the encapsulant browning study was conducted on samples which simulate actual module in the field to increase the reliability of the results.

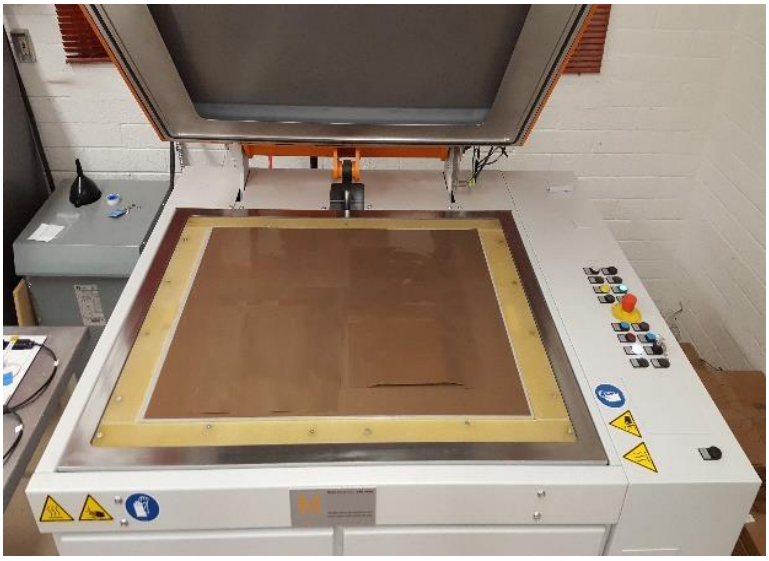

Figure 3.9: Laminator with the cover open

Figure 3.10: Laminator with the control system

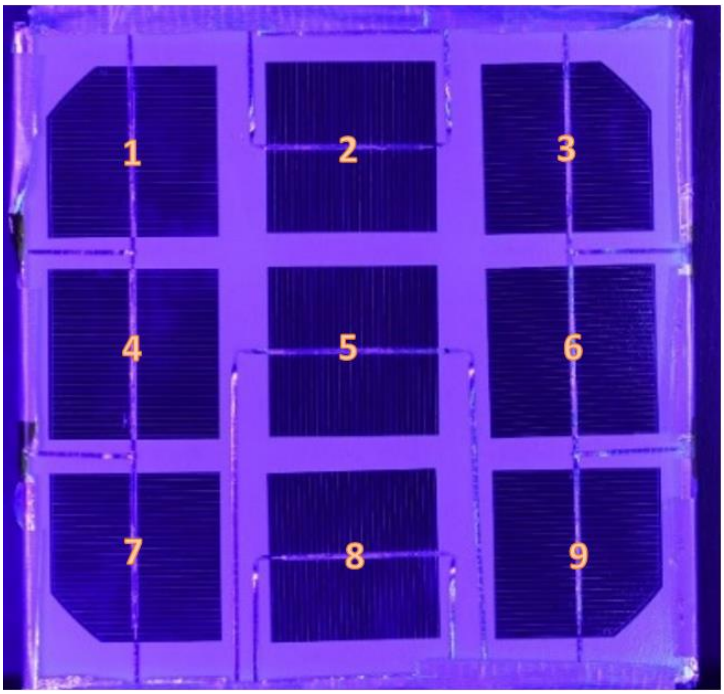

Figure 3.11: Cell numbering scheme in the 9-cell mini-modules (cell pieces cut from a single cell)

3.4 **Characterization Techniques**

3.4.1 **IV Measurement**

The I-V data was collected indoors using the solar simulator. The irradiance monitor on the chuck was calibrated using the PVM 798 reference cell. After calibration, the sample is placed on the chuck. The room temperature is maintained at 25°C. The solar simulator shutter is opened to allow light to fall on the sample and then the measurement is taken. The light IV curve is generated within a second and then the cell is covered to take dark IV measurements. Some of the key IV parameters measured are Isc, open circuit voltage (Voc), fill factor (FF), and Pmax. Isc, Voc and FF of cells in all these mini-modules are

around 1A, 0.6 V and 73%, respectively. Isc is known to be directly proportional to the number of photons incident on the solar cell. Therefore, based on the Isc drop data and exposure time in the weathering chamber, degradation rate was calculated. Pmax drop was not used as it is highly influenced by other IV parameters like Voc and FF from which it would be difficult to isolate the effects of discoloration. For example, fill factor degradation due to solder bond degradation mode is very common in almost all climates and it may affect only power without affecting short-circuit current. Hence, the Isc degradation rate was used in Arrhenius model to estimate activation energy for encapsulant browning.

3.4.2 **UV Fluorescence Imaging**

UV fluorescence imaging is a non-contact and non-destructive method that allows the fast and early detection of the discolored encapsulant, especially during the early stages of yellowing which is not visible to the naked eyes. The UV excitable chromophores present in the yellow region of encapsulant emit fluorescence when irradiated under black/UV light. The imaging setup consists of a visual camera and a UV illumination system comprising of two arrays of 15 UV lamps each inclined at an angle of 45° w.r.t. the module surface (*Figure* Figure *3.12*: (a) Schematic of UVF imaging set-up with two UV light source arrays angled towards the module. The module emits visible light. (b) Photograph of the set-up with the UV arrays.Figure *3.12*). This is done to minimize glare in the visual images due to UV light reflection. Nikon D3400 camera was placed on a tripod stand in between the two arrays and directly facing the module to get a clear image. The setup

provides uniform bright light on the module and this technique provides fast characterization results.

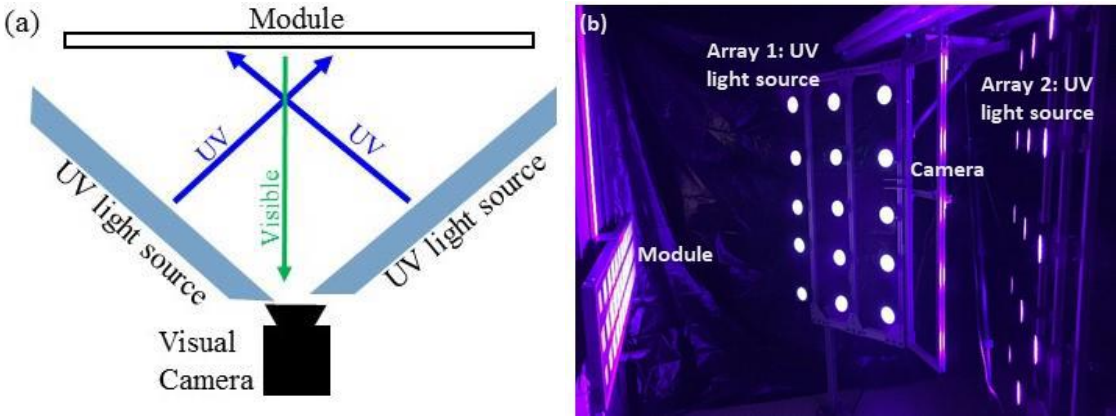

Figure 3.12: (a) Schematic of UVF imaging set-up with two UV light source arrays angled towards the module. The module emits visible light. (b) Photograph of the set-up with the UV arrays.

3.4.3 **Colorimetry Measurement**

The colorimetric measurements were performed on mini-modules to quantify YI by using a calibrated Xrite Ci-60 spectral radiometer. YI is a metric designated to quantitatively measure the change in color of EVA, which could not be seen by naked eye in the initial stage. YI was measured on both sides of the busbar-ribbon in each cell to increase the statistical reliability of collected data as well as to capture any irregularity in the browning pattern. The diameter of the probe is 14 mm which allows measurements to be done close to the cell center. The spectral radiometer is calibrated using white and black reference, which is valid for 24 hours. The change in YI under accelerated stress testing at three

different module temperatures was used in Arrhenius model to calculate the activation energy for encapsulant browning.

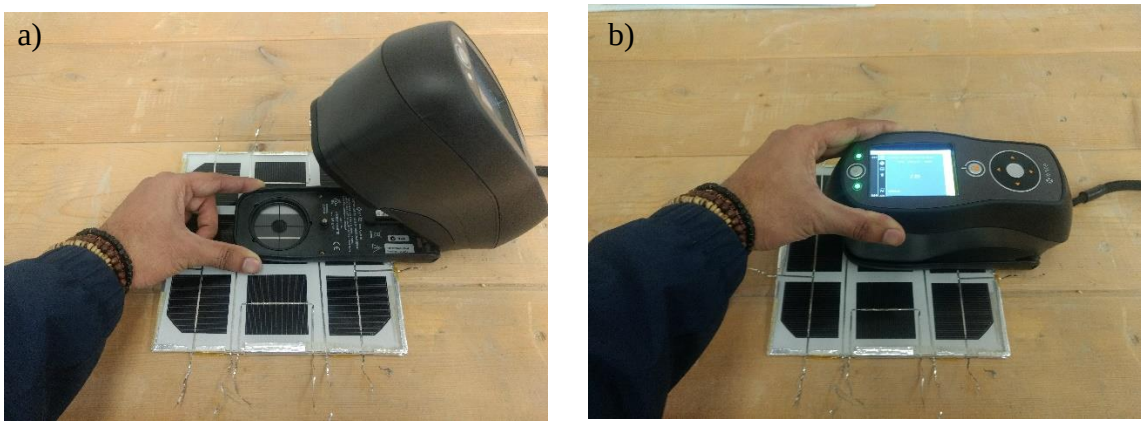

Figure 3.13:Colorimetry setup with a) placing the spectral radiometer and b) taking measurement

3.5 **Model for Activation Energy Estimation**

The Arrhenius model was used to estimate the activation energy from the rate of reaction. In PV context the rate of reaction is considered to be the degradation rate. The model uses degradation rate obtained from accelerated UV testing and module temperature as input parameters. The slope of ln(degradation rate) vs 1/T provides the activation energy of the degradation process.

$$Rate\ of\ reaction = A * e^{\left(\frac{-E_a}{kT}\right)} \tag{3-1}$$

$$ln(rate\ of\ reaction) = \left(\frac{-E_a}{k}\right) * \left(\frac{1}{T}\right) + ln(A) \tag{3-2}$$

where

A is a constant

k = Boltzmann's constant = $8.615 * 10^{-5}$ eV/K

T = Temperature in Kelvin

E_a = Activation energy in eV

4 RESULTS AND DISCUSSION

4.1 UV Fluorescence Results

The UVf results for mini-modules with UV-cut EVA (UVC) and UV-pass EVA (UVP) are discussed in this section.

Figure

Figure *4.1* shows the UVf images of 3 mini-modules with UV-cut EVA taken at different stages of UV exposure testing. After 200 kWh/m^2 of UV dosage, there is yellowing at the cell center but not at the cell edges in the modules with oxygen diffusion-prevented backsheet. In the test module, the cell area is hotter than the inter-cell area because of solar gain in the semiconductor material due to thermalization effect. It seems the acetic acid, a catalyst for encapsulant discoloration, as shown in *Figure Figure 1.1*, formed at the hot cell center does not diffuse to the cool inter-cell area whereas the acetic acid formed at the hot cell edges diffuse to the inter-cell area. The change in color is more pronounced in modules operating at a higher temperature. This indicates that the degradation rate, as expected, aggravates with increase in temperature. The yellowing is further enhanced with longer UV exposure of 400 kWh/m^2. This indicates UV dosage is an important factor in encapsulant degradation.

Figure Figure *4.2* shows the UVf images of 3 mini-modules with UV-pass EVA taken at different stages of UV exposure testing. It shows no yellowing over the cell area or the non-cell area. However, a complete delamination of encapsulant was observed over the cell area in UVf but not in visual inspection. This effect was more pronounced in the mini-

module operating at higher temperatures and becomes more noticeable in the third stage of UVf images. The delamination could be due to the different or no adhesion promoting additives used in the EVA. The results infer that UVf technique also has the capability to detect delamination in module at a very early stage of the issue.

UV-cut Mini-module	UV dosage		
	0 kWh/m^2	200 kWh/m^2	400 kWh/m^2
UVC-1 (Low T) 64°C	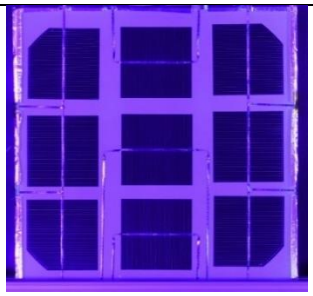		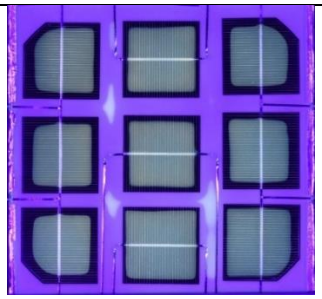
UVC-2 (Mid T) 73°C	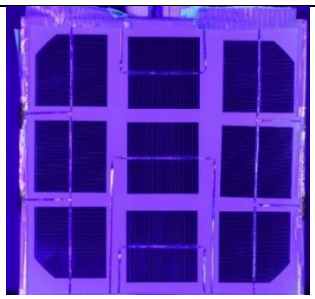	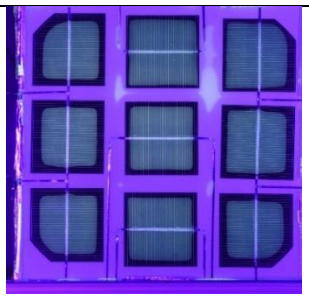	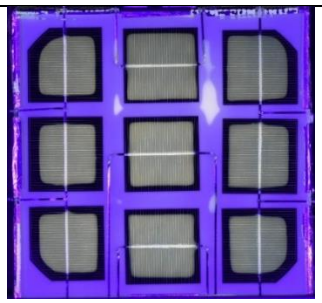
UVC-3 (High T) 78°C	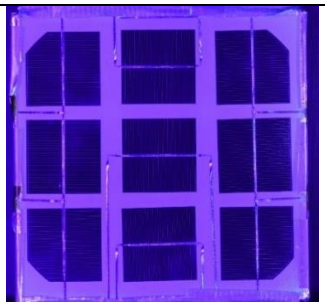	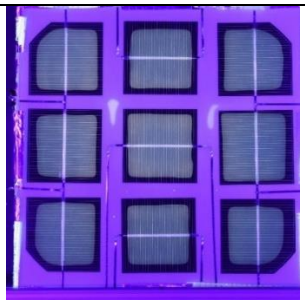	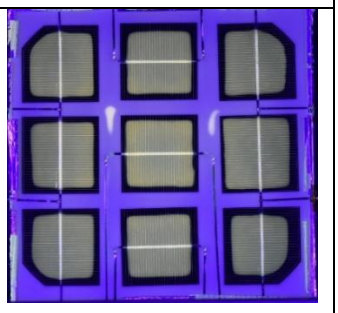

Figure 4.1: UVf images of UVC mini-modules at different temperatures and UV dosage levels under accelerated UV testing.

UV-pass Mini-module	UV dosage		
	0 kWh/m^2	200 kWh/m^2	400 kWh/m^2
UVP-1 (Low T) 64°C	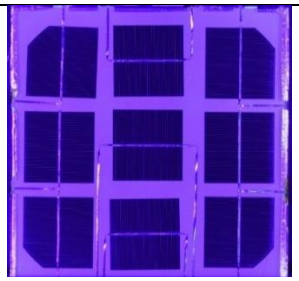	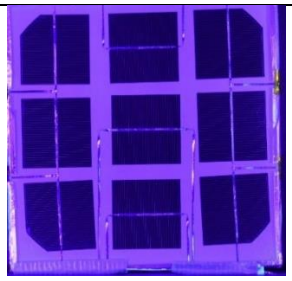	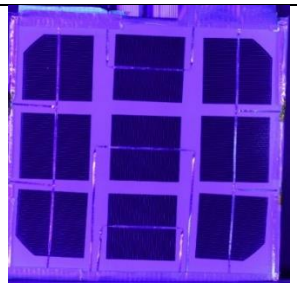
UVP-2 (Mid T) 73°C	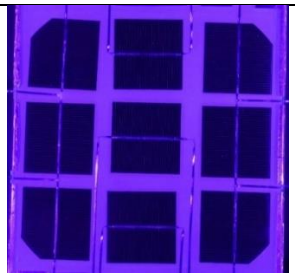	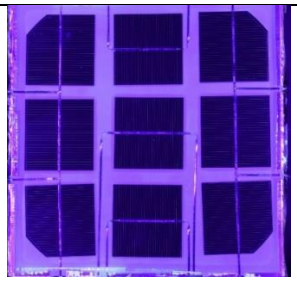	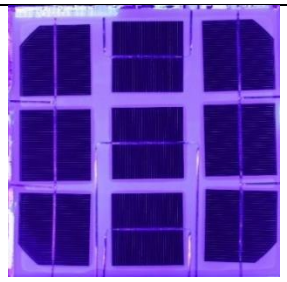
UVP-3 (High T) 78°C	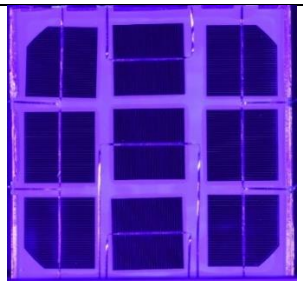	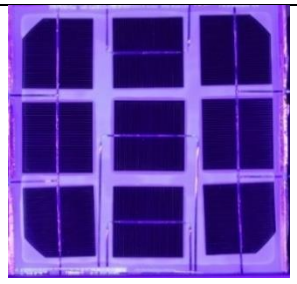	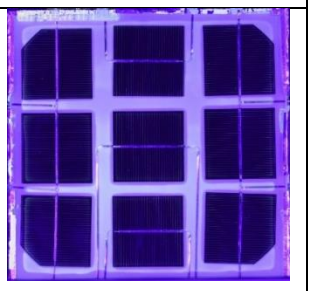

Figure 4.2: UVf images of UVP mini-modules at different temperatures and UV dosage levels under accelerated UV testing.

UV dosage		
0 kWh/m^2	200 kWh/m^2	400 kWh/m^2
Center cell from mini-module with UV-cut EVA (UVC-3) (high temperature)		
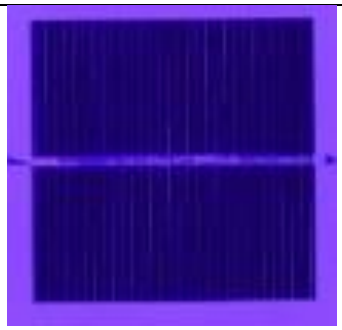	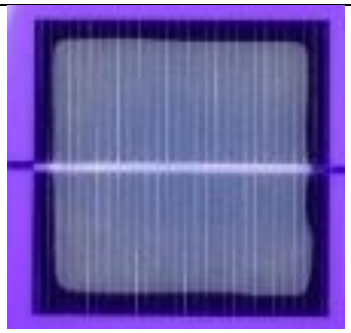	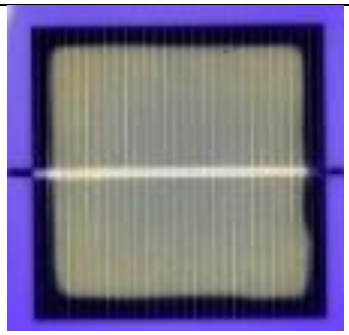
Center cell from mini-module with UV-pass EVA (UVP-3) (high temperature)		
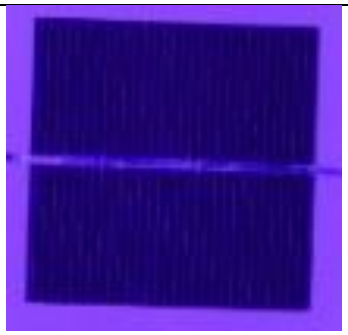	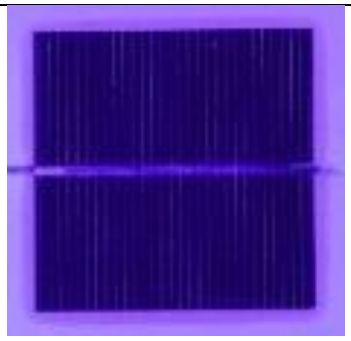	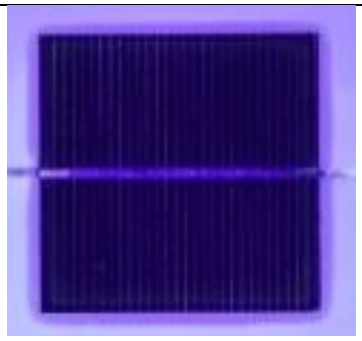

Figure 4.3: Close-up UVf images of center cell from UVC-3 (high temperature) and UVP-3 (high temperature) modules

4.2 **IV Results**

The IV measurements were done for all six UV-stressed mini-modules along with two control modules. These mini-modules were tested using a solar simulator at STC to obtain their electrical parameters. The initial Isc, Voc and FF of cells in all these mini-modules are around 1A, 0.6 V and 73%, respectively. The IV plots for one of the cells at different stages of the test are shown in *Figure* Figure *4.4* and *Figure* Figure *4.5*.

Encapsulant yellowing causes a reduction in Isc due to loss in transmission of light to the solar cells. Isc drop is higher in the UVC module operating at higher temperature as shown in *Figure* Figure *4.6* and even higher drop is seen with increased exposure to UV stress as shown in *Figure* Figure *4.4*. These results support the UVf findings, where more browning was seen after increased UV exposure in UVC modules operating at higher temperatures. It also demonstrates that the UVf imaging technique is a powerful tool to detect the early sign of discoloration, which is neither visible to the naked eyes nor fully quantified by Isc loss.

On the other hand, the Isc loss is significantly higher at low temperature for the UVP modules as compared to the UVC modules and also, more importantly, is nearly the same for the UVP modules irrespective of temperatures indicating that the optical decoupling due to delamination is nearly the same irrespective of its severity. These results support the

UVf findings from chapter **Error! Reference source not found.**, which showed no browning in these modules but clear evidence of delamination.

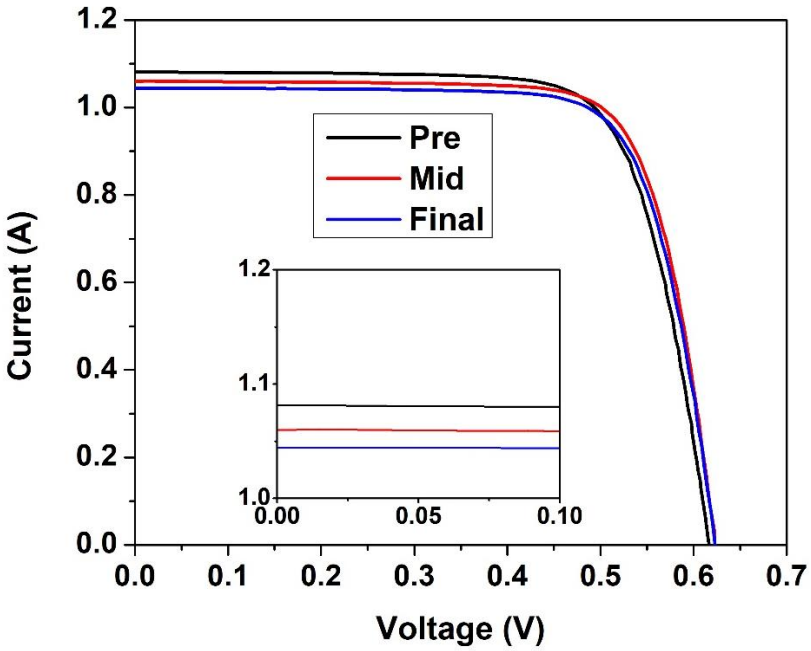

Figure 4.4: IV curve for UVC-3 cell 2 at various stages of accelerated stress test (0, 200 and 400 kWh/m^2 UV dosage)

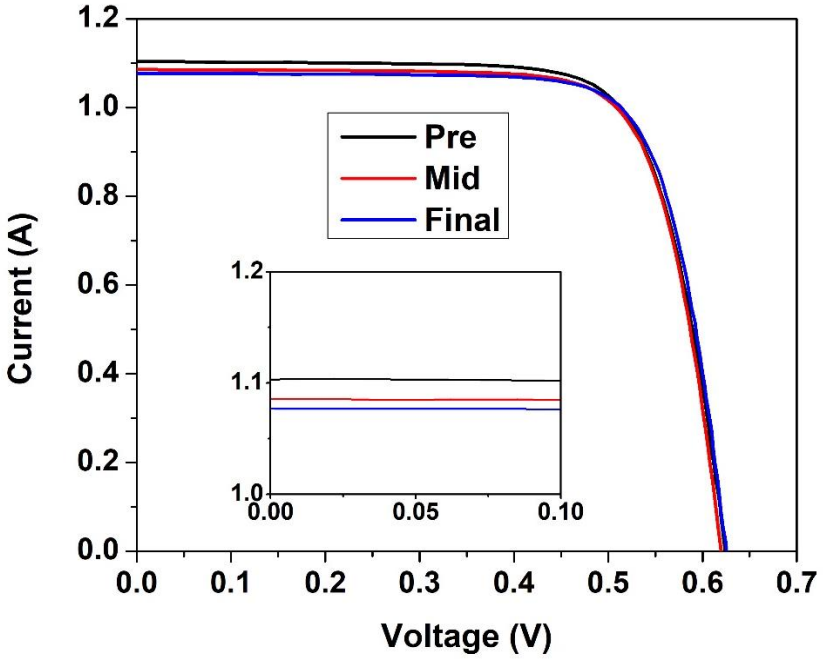

Figure 4.5: IV curve for UVP-3 cell 2 at various stages of accelerated stress test (0, 200 and 400 kWh/m^2 UV dosage)

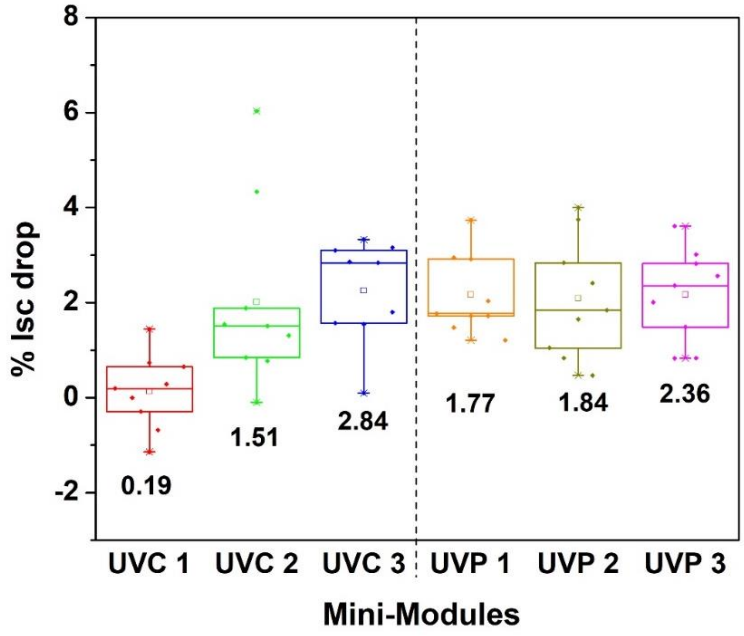

Figure 4.6: Percent Isc degradation of mini-modules after 400 kWh/m^2 UV exposure in the chamber testing at low (UVC 1, UVP 1), mid (UVC 2, UVP 2) and high (UVC 3, UVP 3) temperatures.

4.3 **Colorimetry Results**

The ΔYI values for all the mini-modules with UV cut EVA are shown in Figure *4.7*. There is a significant change in YI values in comparison with the control module, not undergoing a stress test. ΔYI of all UVC modules is positive and increases with the increase in module temperature. It confirms the occurrence of yellowing, which is in close correspondence with the UVf results.

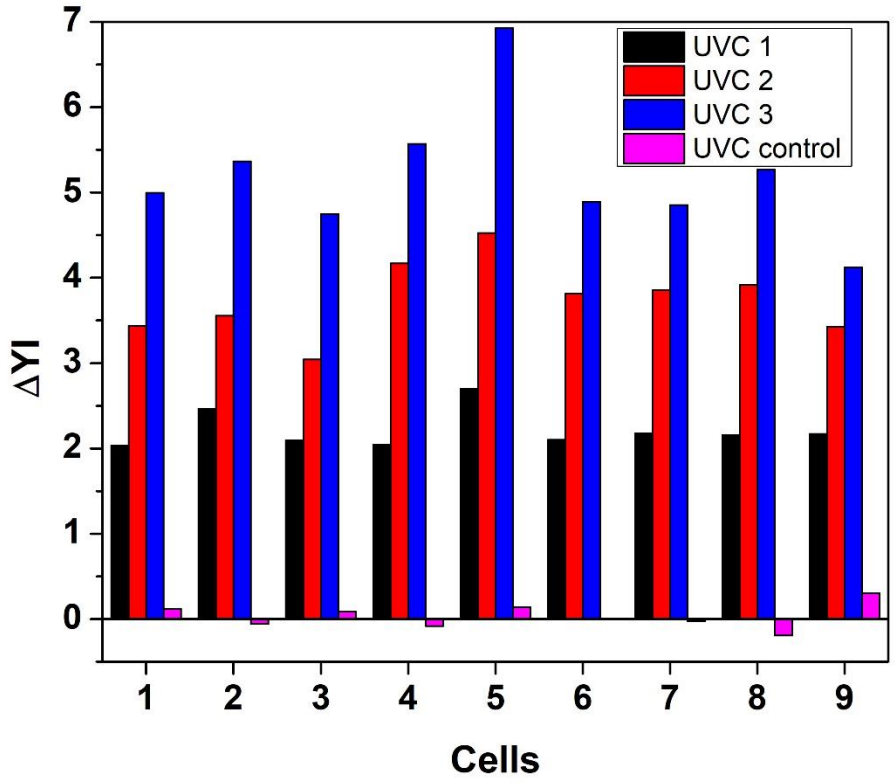

Figure 4.7: ΔYI values for cells of different UVC modules along with control module (UVC 1 low temperature; UVC 2 mid temperature; UVC 3 high temperature)

The ΔYI values for all the mini-modules with UV-pass EVA are shown in *Figure* Figure *4.8*. ΔYI values of all UVP modules are negligibly small and close to the values for control module. This indicates that there is not much change in color in these modules over or between the cells. These results are in close correspondence with the UVf results, where images show no significant change in color.

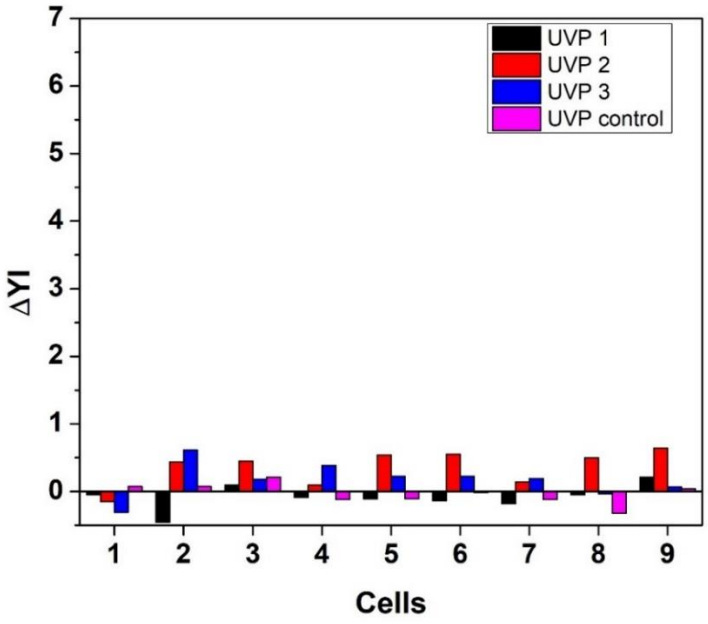

Figure 4.8: ΔYI values for cells of different UVP modules along with control module (UVP 1 low temperature; UVP 2 mid temperature; UVP 3 high temperature)

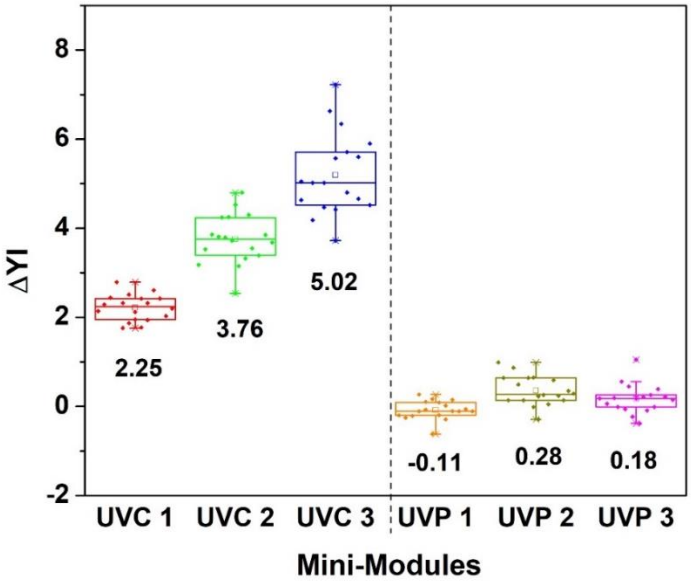

Figure 4.9: ΔYI of mini-modules after 400 kWh/m^2 UV exposure in the chamber testing at low (UVC 1, UVP 1), mid (UVC 2, UVP 2) and high (UVC 3, UVP 3) temperatures.

Table 4-1: Characterization results for center cell of all UVC modules

UV-cut mini-module	UV dosage		
	0 kWh/m^2	200 kWh/m^2	400 kWh/m^2
UVC-1 (Low T) 64°C	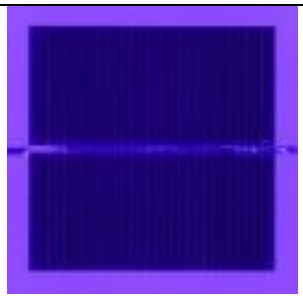 Isc= 1.066 A YI= -4.92	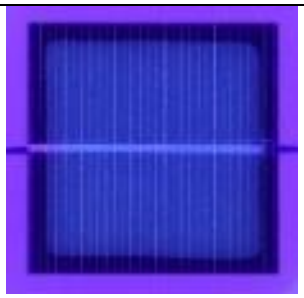 Isc= 1.064 A YI= -3.74	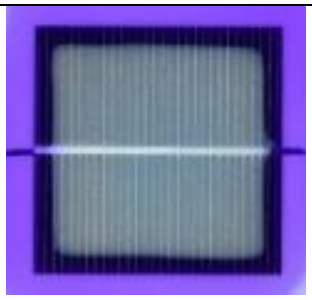 Isc= 1.066 A YI=-2.22
UVC-2 (Mid T) 73°C	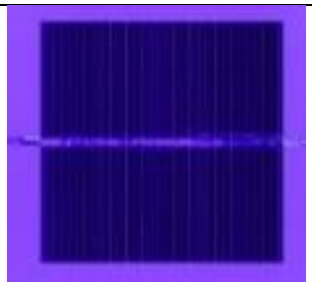 Isc= 1.063 A YI= -3.32	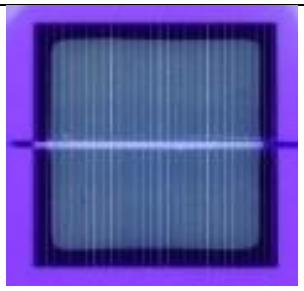 Isc= 1.056 A YI= -1.67	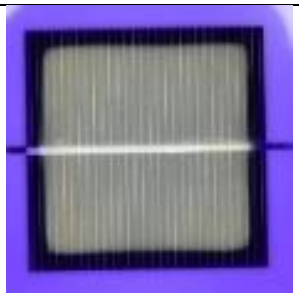 Isc= 1.054 A YI= 1.21
UVC-3 (High T) 78°C	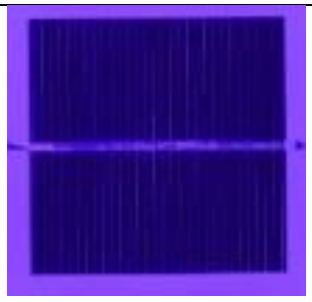 Isc= 1.065 A YI= -4.53	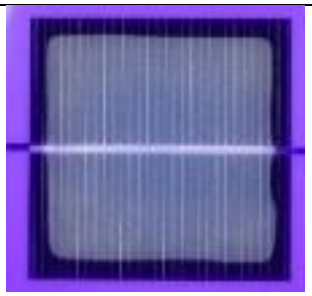 Isc= 1.043 A YI= -2.28	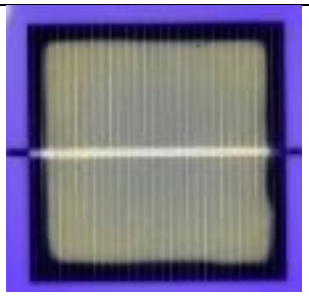 Isc= 1.032 A YI= 2.40

Table 4-2: Characterization results for center cell of all UVP modules

UV-pass mini-module	UV dosage		
	0 kWh/m^2	200 kWh/m^2	400 kWh/m^2
UVP-1 (Low T) 64°C	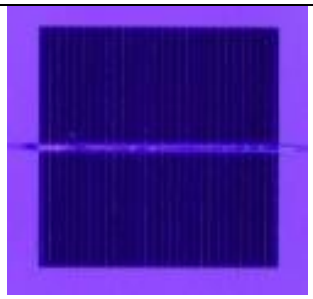 Isc= 1.075 A YI= -3.20	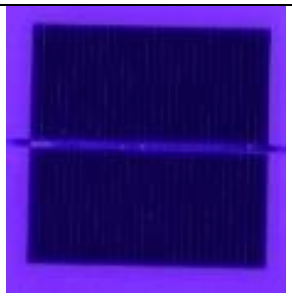 Isc= 1.071 A YI= -3.44	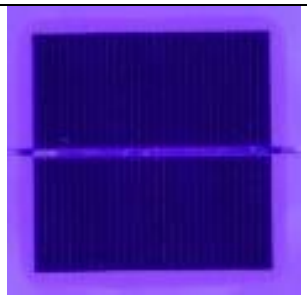 Isc= 1.062 A YI=-3.31
UVP-2 (Mid T) 73°C	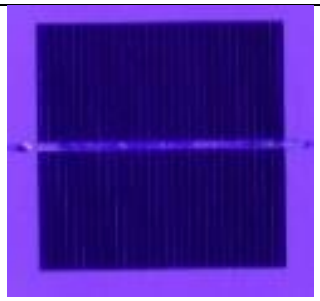 Isc= 1.067 A YI= -3.19	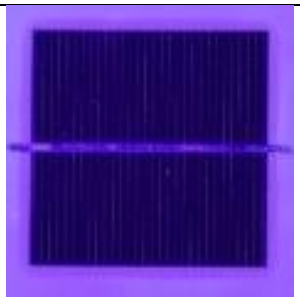 Isc= 1.068 A YI= -2.87	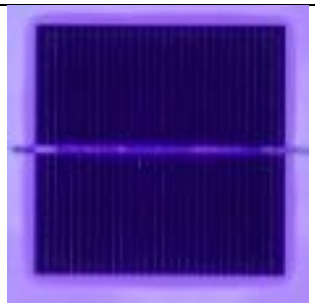 Isc= 1.062 A YI= -2.65
UVP-3 (High T) 78°C	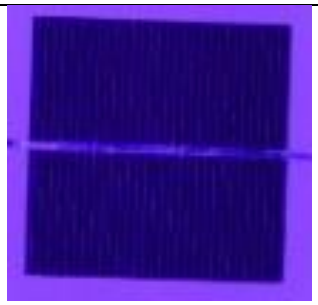 Isc= 1.078 A YI= -4.39	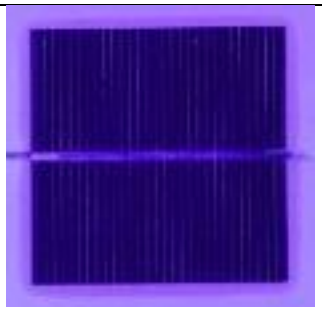 Isc= 1.077 A YI= -4.46	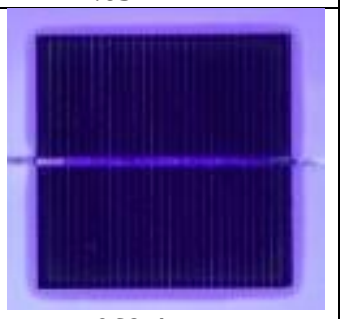 Isc= 1.069 A YI= -4.16

In summary, UVf technique provides visual evidence of discoloration in mini-modules with UV-cut EVA and traces of delamination in mini-modules with UV-pass EVA at the very early stage of the issues. It is also verified from YI data.

4.4 Correlation between Isc and YI

It should be noted that there is limited correlation between Isc and YI in UVC modules (*Figure* Figure *4.10*). This could be attributed to the fact that Isc is dictated by both yellowed (at the cell center) and non-yellowed (cell edges) areas whereas YI is measured only at the yellowed area at the center. So, only limited linear correlation exists when yellowing is extremely minimal and can be detected only by UVf method, not by naked eyes or visual camera. The mini-module operating at the lowest temperature (UVC-1) shows a very different behavior than other mini-modules. This could be attributed to very low degradation at lower temperature due to which Isc values do not change significantly and are within the measurement error.

However, if a field aged browned module is used (no acetic acid is expected to be left out to catalyze the discoloration rate), it is anticipated that the YI and Isc would have a good linear correlation as all the acetic acid on the cell surface is either consumed (cell center) or driven out (cell edges).

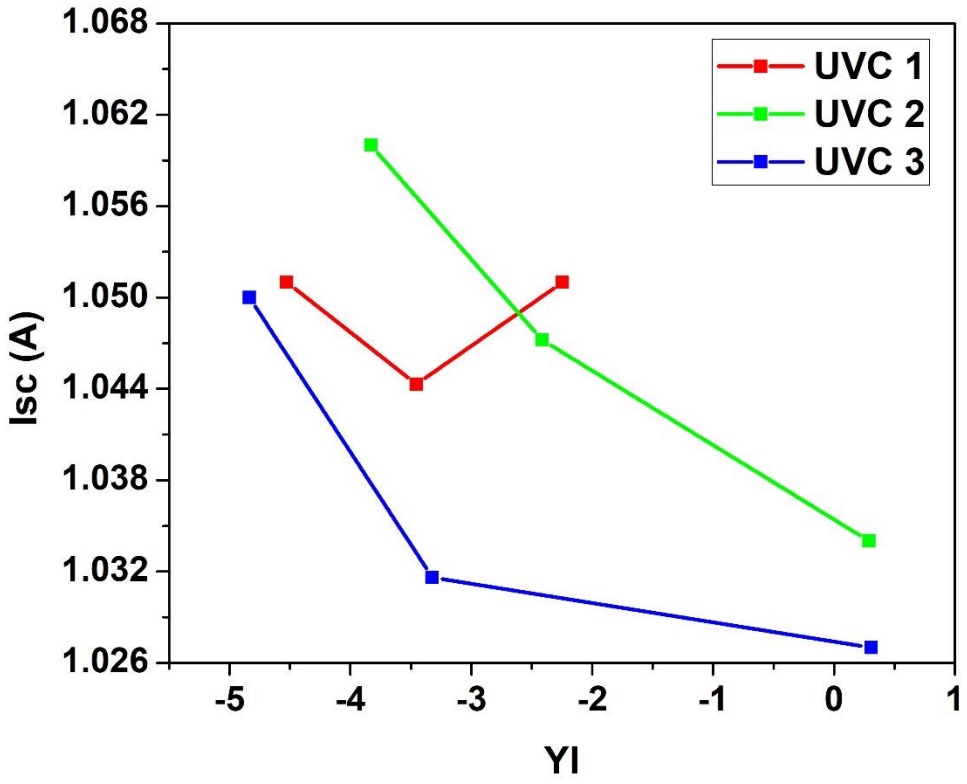

Figure 4.10: Isc vs YI plot for UVC modules at various stages of the accelerated stress test

There is no significant change in the YI values while Isc values dropped significantly for UVP modules as seen in *Figure* Figure *4.11*. There is no correlation between Isc and YI for UVP modules as the EVA does not undergo yellowing but the interface between cell front-surface and EVA is clearly delaminated as observed in UVf study in section 4 above. The delamination severely affects Isc but not the YI. Therefore, no correlation could be expected between Isc loss and YI increase.

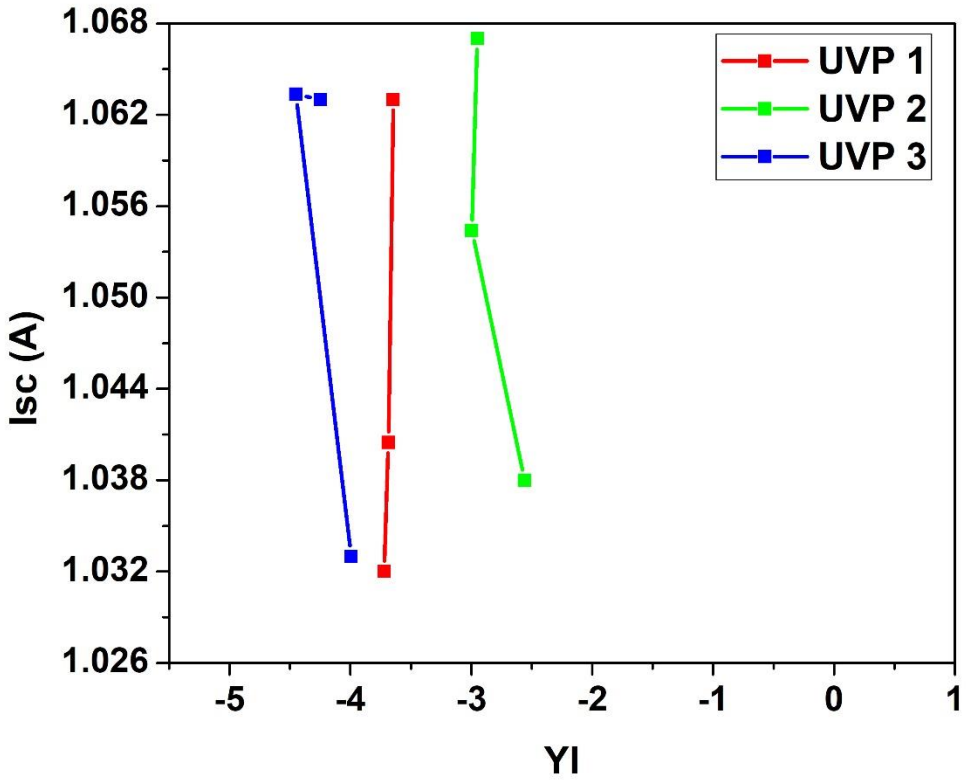

Figure 4.11: Isc vs YI plot for UVP modules at various stages of the accelerated stress test

4.5 **Activation Energy Determination**

The activation energy for encapsulant discoloration was determined by two different approaches using Arrhenius model: cell Isc degradation and change in YI.

3.6.1 **Activation Energy Calculation from Isc Drop**

A linear regression model is fitted in the plot of %Isc drop and module temperature in the stress testing as shown in Figure *4.12*. The slope of ln(% Isc drop) vs 1/T plot in *Figure* Figure *4.12* is $-E_a/k$. E_a is estimated from the slope and the value is 0.82 eV.

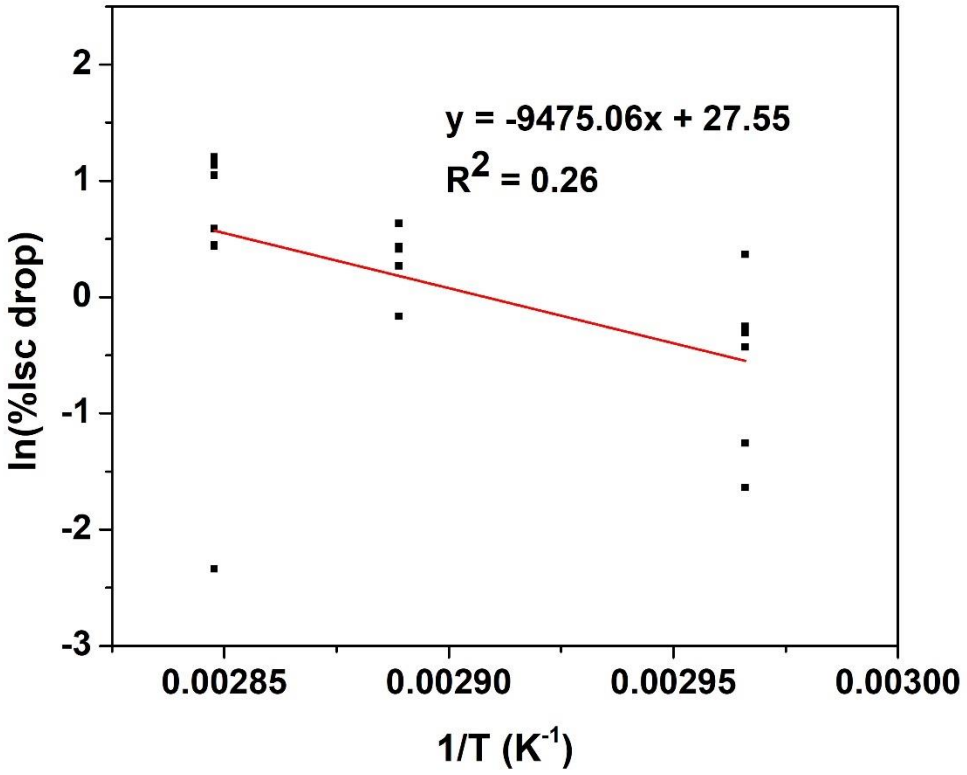

Figure 4.12: Variation of ln(Isc drop(%)) of UVC modules with inverse of temperature. Activation energy is calculated from the slope of linear fit on degradation data at three different temperatures.

3.6.2 **Activation Energy Calculation from YI Data**

A linear regression model is fitted in the plot of *ΔYI* and inverse of module temperature in the stress testing as shown in *Figure* Figure 4.13. The slope of ln(*ΔYI*) vs 1/T plot in Figure 4.13 is $-E_a/k$. E_a is estimated from the slope and the value is 0.61eV.

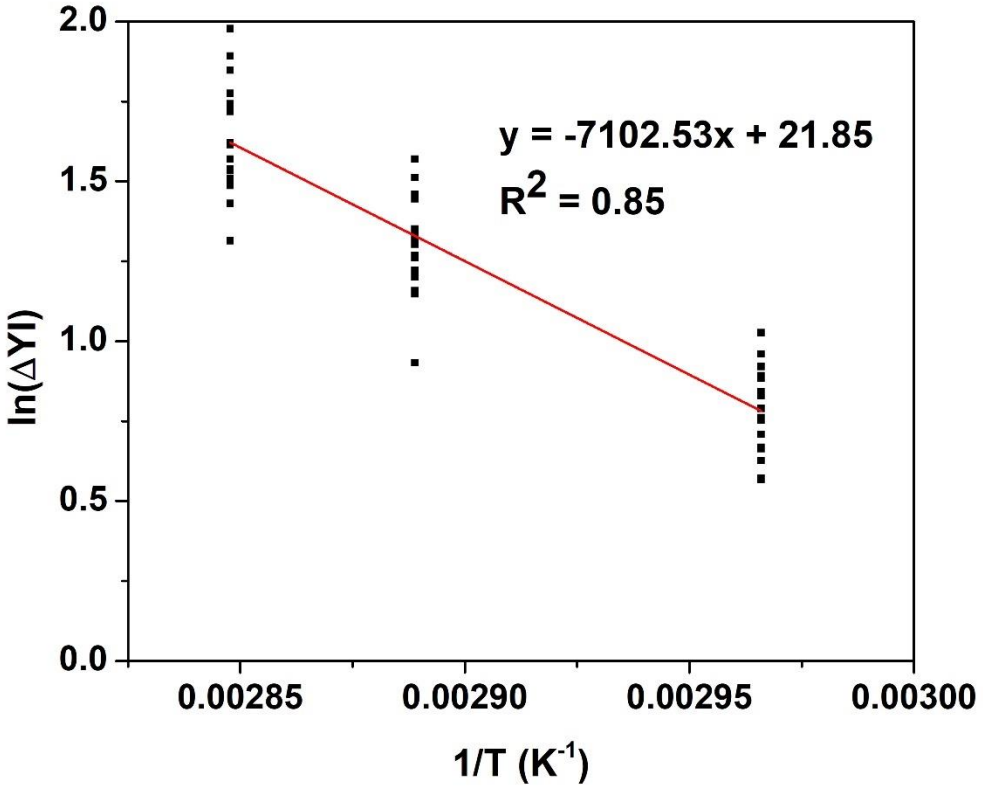

Figure *4.13:* Variation of ln(ΔYI) of UVC modules with inverse of temperature. Activation energy is calculated from the slope of linear fit on degradation data at three different temperatures.

The reason for the difference in E_a values estimated from Isc drop and from ΔYI is that the Isc is dictated by whole cell area (yellowed and non-yellowed region) while YI is taken only at the yellowed region. This also infers that YI provides better estimation of activation energy for encapsulant browning compared to that from the cell Isc drop if the encapsulant layer over the cell has both yellowed and non-yellowed regions. The cell Isc drop can also be used to accurately determine Ea values if the Isc value is measured only at the cell center using a black mask or is normalized for the yellowed and non-yellowed areas and intensities using an image processing technique.

5 CONCLUSIONS

An indoor accelerated UV testing was performed on mini-modules with UV-cut and UV-pass EVA while blocking the oxygen diffusion and maintaining at three different temperatures in a single chamber run.

- UVf technique provides visual evidence of encapsulant discoloration in mini-modules with UV-cut EVA and traces of delamination in mini-modules with UV-pass EVA at the very early stage of the issues. It is also verified from YI data (Table *5-1* and Table *5-2*).
- For UVC modules, Isc drop increases with a rise in module operating temperature. On the other hand, the Isc loss is nearly the same for UVP modules irrespective of the module operating temperature indicating that the optical decoupling due to delamination is nearly the same irrespective of the severity of temperature.
- Only limited correlation is seen between Isc and YI in UVC modules as Isc is dictated by both yellowed (at the cell center) and non-yellowed (cell edges) areas whereas YI is measured only by the yellow area at the center. However, a good linear correlation could probably be established using the following four approaches: 1) measure Isc only in the yellowed area using a mask to illuminate only the desired area; 2) measure quantum efficiency (QE) only in the yellowed area; 3) use an image processing technique to obtain yellowness index (YI) / browning index (BI) for the entire cell, not just at the cell center; 4) start the UV

stress test on the module which is already visually browned in the field or in the accelerated UV test.

- No correlation is seen between Isc and YI in UVP modules, which was expected, as this material does not undergo yellowing but the interface between cell front-surface and EVA is clearly delaminated as observed in the UVf study. The delamination severely affects Isc but not the YI.
- The activation energy for encapsulant discoloration was determined by two different approaches using Arrhenius model: cell Isc drop and change in YI. Ea estimated from Isc drop is 0.82 eV while from YI is 0.61 eV. The reason for the difference is that the Isc is dictated by whole cell area (yellowed and non-yellowed region) while YI is taken only at the yellowed region. This also infers that YI provides a better estimation of activation energy compared to that from the cell Isc drop especially when the discoloration is only at the cell center and could not be seen by naked eyes. To improve the estimation of activation energy from Isc drop, a small mask could be used so that IV measurement is done only over the yellowed region.
- The determination of activation energy allows lifetime prediction of modules in different climatic condition. This accelerated UV testing approach can be replicated to the commercial size modules and consumes less time and resources.

Table 5-1: Characterization results for center cell of all UVC modules

UV-cut mini-module	UV dosage		
	0 kWh/m^2	200 kWh/m^2	400 kWh/m^2
UVC-1 (Low T) 64°C	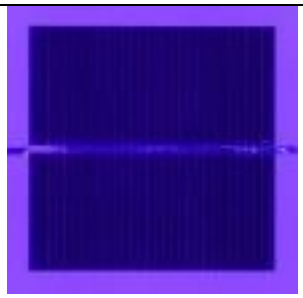 Isc= 1.066 A YI= -4.92	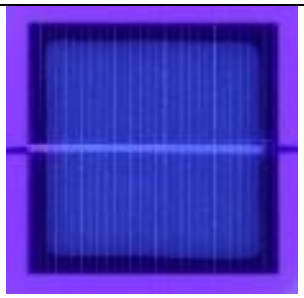 Isc= 1.064 A YI= -3.74	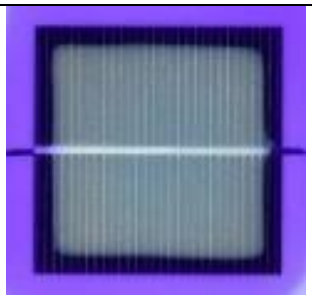 Isc= 1.066 A YI=-2.22
UVC-2 (Mid T) 73°C	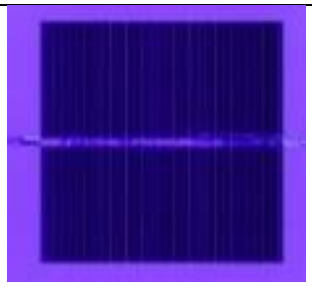 Isc= 1.063 A YI= -3.32	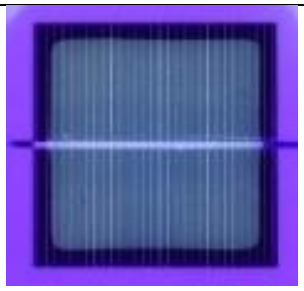 Isc= 1.056 A YI= -1.67	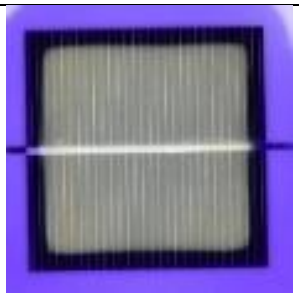 Isc= 1.054 A YI= 1.21
UVC-3 (High T) 78°C	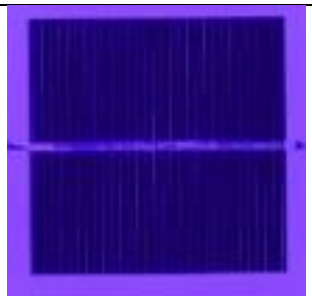 Isc= 1.065 A YI= -4.53	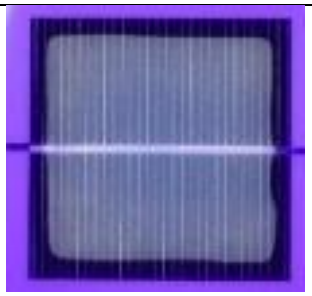 Isc= 1.043 A YI= -2.28	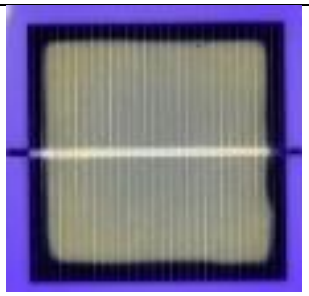 Isc= 1.032 A YI= 2.40

Table 5-2:Characterization results for center cell of all UVP modules

UV-pass mini-module	UV dosage		
	0 kWh/m^2	200 kWh/m^2	400 kWh/m^2
UVP-1 (Low T) 64°C	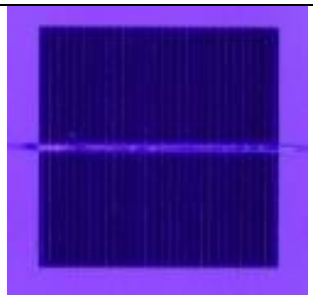 Isc= 1.075 A YI= -3.20	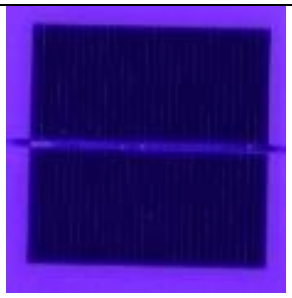 Isc= 1.071 A YI= -3.44	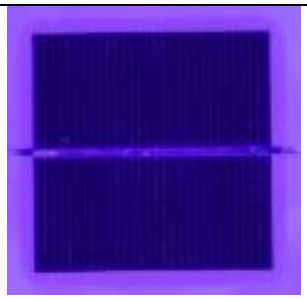 Isc= 1.062 A YI=-3.31
UVP-2 (Mid T) 73°C	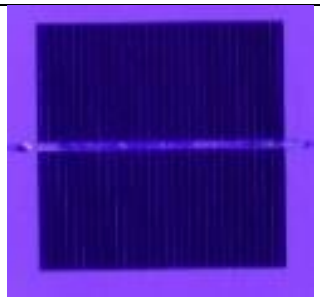 Isc= 1.067 A YI= -3.19	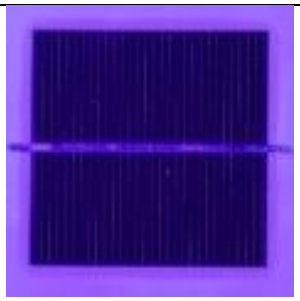 Isc= 1.068 A YI= -2.87	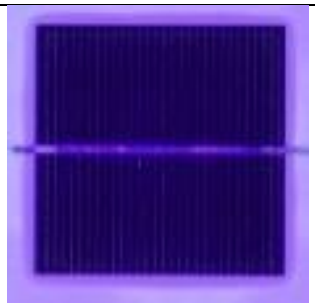 Isc= 1.062 A YI= -2.65
UVP-3 (High T) 78°C	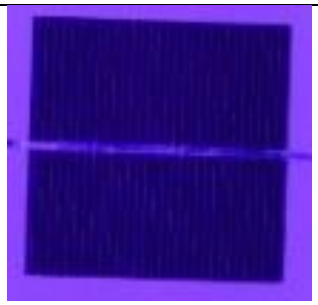 Isc= 1.078 A YI= -4.39	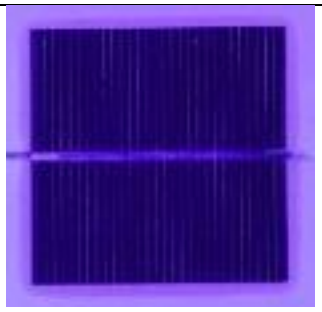 Isc= 1.077 A YI= -4.46	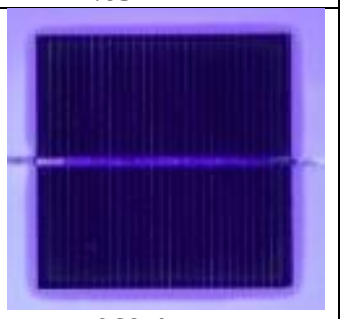 Isc= 1.069 A YI= -4.16

REFERENCES

[1] A. A. Suleske, “Performance Degradation of Grid-Tied Photovoltaic Modules in a Desert Climatic Condition,” Masters Thesis, Arizona State University, 2010.

[2] K. Agroui, M. Jaunich, and A. H. Arab, “Analysis Techniques of Polymeric Encapsulant Materials for Photovoltaic Modules: Situation and Perspectives,” *Energy Procedia*, vol. 93, no. March, pp. 203–210, 2016.

[3] A. W. Czanderna and F. J. Pern, “Encapsulation of PV modules using ethylene vinyl acetate copolymer as a pottant: A critical review,” *Sol. Energy Mater. Sol. Cells*, vol. 43, no. 2, pp. 101–181, 1996.

[4] F. Pern, “Ethylene vinyl acetate (EVA) encapsulants for photovoltaic modules: Degradation and discoloration mechanisms and formulation modifications for improved,” *Die Angew. Makromol. Chemie*, vol. 252, pp. 195–216, 1997.

[5] D. E. Ellibee, B. R. Hansen, D. L. King, J. A. Kratochvil, and M. A. Quintana, “Photovoltaic module performance and durability following long-term field exposure,” 1998.

[6] M. Köntges *et al.*, *Assessment of Photovoltaic Module Failures in the Field*. 2017.

[7] F. J. Pern and S. H. Glick, “Fluorescence analysis as a diagnostic tool for polymer encapsulation processing and degradation,” *AIP Conf. Proc.*, vol. 306, pp. 573–585, 1994.

[8] “Energy of activation,” 2011. [Online]. Available: http://www.mitchellroth.com/wp-content/uploads/2011/04/Energy-of-Activation.gif. [Accessed: 20-Aug-2003].

[9] A. Sinha, O. S. Sastry, and R. Gupta, “Nondestructive characterization of encapsulant discoloration effects in crystalline-silicon PV modules,” *Sol. Energy Mater. Sol. Cells*, vol. 155, pp. 234–242, 2016.

[10] J. C. Schlothauer, K. Grabmayer, I. Hintersteiner, G. M. Wallner, and B. Röder, “Non-destructive 2D-luminescence detection of EVA in aged PV modules: Correlation to calorimetric properties, additive distribution and a clue to aging parameters,” *Sol. Energy Mater. Sol. Cells*, vol. 159, pp. 307–317, 2017.

[11] P. Klemchuk, M. Ezrin, G. Lavigne, W. Holley, J. Galica, and S. Agro, “Investigation of the degradation and stabilization of EVA-based encapsulant in field-aged solar energy modules,” *Polym. Degrad. Stab.*, vol. 55, no. 3, pp. 347–365, 1997.

[12] C. Peike, L. Purschke, K. A. Weiss, M. Kohl, and M. Kempe, “Towards the origin of photochemical EVA discoloration,” *Conf. Rec. IEEE Photovolt. Spec. Conf.*, pp.

1579–1584, 2013.

[13] B.-Å. Sultan and E. Sörvik, “Thermal degradation of EVA and EBA—A comparison. I. Volatile decomposition products,” *J. Appl. Polym. Sci.*, vol. 43, no. 9, pp. 1737–1745, Nov. 1991.

[14] U. Weber *et al.*, “Acetic acid production, migration and corrosion effects in ethylene-vinyl-acetate-(EVA) based PV modules.,” in *27th EUPVSEC*, 2012, pp. 2992–2995.

[15] K. Thaworn, “Effects of Organic Peroxides on the Curing Behavior of EVA Encapsulant Resin,” *Open J. Polym. Chem.*, vol. 2, no. 2, pp. 77–85, 2012.

[16] J. L. Hodgson and M. L. Coote, “Clarifying the Mechanism of the Denisov Cycle: How do Hindered Amine Light Stabilizers Protect Polymer Coatings from Photo-oxidative Degradation?,” *Macromolecules*, vol. 43, no. 10, pp. 4573–4583, May 2010.

[17] P. Bortolus, N. Camaioni, L. Flamigni, F. Minto, S. Monti, and A. Faucitano, “Photostabilization mechanisms of hindered amine light stabilizers: interaction of singlet and triplet anthracene with piperidine model compounds,” *J. Photochem. Photobiol. A Chem.*, vol. 68, no. 2, pp. 239–246, Sep. 1992.

[18] F. J. Pern, “Factors that affect the EVA encapsulant discoloration rate upon accelerated exposure,” *Sol. Energy Mater. Sol. Cells*, vol. 41–42, pp. 587–615, Jun. 1996.

[19] A. Morlier *et al.*, “Influence of the curing state of ethylene-vinyl acetate on photovoltaic modules aging,” in *28th EUPVSEC*, 2013, pp. 2832–2837.

[20] D. C. Miller *et al.*, “Degradation in PV encapsulant strength of attachment: An interlaboratory study towards a climate-specific test,” *Conf. Rec. IEEE Photovolt. Spec. Conf.*, vol. 2016–Novem, pp. 95–100, 2016.

[21] D. J. V. Kumar, “Determination of Activation Energy for Encapsulant Browning of Photovoltaic Modules,” Masters Thesis, Arizona State University, 2016.

[22] S. Pore, “Reliability of PV Modules : Dependence on Manufacturing Quality and Field Climatic Conditions,” Masters Thesis, Arizona State University, 2017.

[23] P. Sánchez-Friera, M. Piliougine, J. Peláez, J. Carretero, and M. Sidrach de Cardona, “Analysis of degradation mechanisms of crystalline silicon PV modules after 12 years of operation in Southern Europe,” *Prog. Photovoltaics Res. Appl.*, vol. 19, no. 6, pp. 658–666, Sep. 2011.

[24] A. Sinha, O. S. Sastry, and R. Gupta, “Detection and characterisation of delamination in PV modules by active infrared thermography,” *Nondestruct. Test. Eval.*, vol. 31, no. 1, pp. 1–16, Jan. 2016.

[25] Y. Voronko *et al.*, “Long term performance of pv modules: System optimization through the application of innovative non-destructive characterization methods,” *27th Eur. Photovolt. Sol. Energy Conf. Exhib.*, no. October, pp. 3530–3535, 2012.